Memoirs of the Queensland Museum | **Nature**

59

PO Box 3300, South Brisbane 4101, Australia
Phone 06 7 3840 7555
Fax 06 7 3846 1226
Email qmlib@qm.qld.gov.au
Website www.qm.qld.gov.au

National Library of Australia card number
ISSN 2204-1478 (Online)
ISSN 0079-8835 (Print)

NOTE

Papers published in this volume and in all previous volumes of the *Memoirs of the Queensland Museum* may be reproduced for scientific research, individual study or other educational purposes. Properly acknowledged quotations may be made but queries regarding the republication of any papers should be addressed to the Director. Hard copies of the journal can be purchased from the Queensland Museum Shop or are freely available online through the museum website.

A Guide to Authors is displayed at the Queensland Museum web site www.qm.qld.gov.au

A Queensland Government Project
Typeset at the Queensland Museum

A taxonomic assessment of the Australian Dusky Antechinus Complex: a new species, the Tasman Peninsula Dusky Antechinus (*Antechinus vandycki* sp. nov.) and an elevation to species of the Mainland Dusky Antechinus (*Antechinus swainsonii mimetes* (Thomas))

Baker, A.M.

Queensland University of Technology, 2 George Street, Brisbane, Qld, 4001, Australia. Corresponding Author Email: am.baker@qut.edu.au

Queensland Museum, PO Box 3300, South Brisbane Qld 4101

Mutton, T.Y.

Mason, E.D.

Gray, E.L.

Queensland University of Technology, 2 George Street, Brisbane, Qld 4001 Australia.

Citation. Baker, A.M., Mutton, T.Y., Mason, E.D. & Gray, E.L. 2015. A taxonomic assessment of the Australian Dusky Antechinus Complex: a new species, the Tasman Peninsula Dusky Antechinus (*Antechinus vandycki* sp. nov.) and an elevation to species of the Mainland Dusky Antechinus (*Antechinus swainsonii mimetes* (Thomas)). *Memoirs of the Queensland Museum – Nature* 59: 75-126. Brisbane. ISSN 2204-1478 (Online), ISSN 0079-8835 (Print). Accepted: 25 November 2014. First published online: 26 May 2015.

http://dx.doi.org/10.17082/j.2204-1478.59.2015.2014-10

LSID - lsid:zoobank.org:pub:0FC36E36-D655-4C82-A356-519105200E83

ABSTRACT

In 2014, the northern outlying population of carnivorous marsupial Dusky Antechinus (*Antechinus swainsonii*) was nominated a new species, *A. arktos*. Here, we describe a further new species in the dasyurid *A. swainsonii* complex, which now contains five taxa. We recognise two distinct species from Tasmania, formerly represented by *A. swainsonii swainsonii* (Waterhouse); one species (and 2 subspecies) from mainland south-eastern Australia, formerly known as *A. swainsonii mimetes* (Thomas) and *A. swainsonii insulanus* Davison; and one species from the Tweed Caldera in mid-eastern Australia, formerly known as *A. s. mimetes* but recently described as *A. arktos* Baker, Mutton, Hines and Van Dyck. Primacy of discovery dictates the Tasmanian Dusky Antechinus *A. swainsonii* (Waterhouse) is nominate; the Mainland Dusky Antechinus taxa, one raised from subspecies within *A. swainsonii mimetes* (Thomas) is elevated to species (now *A. mimetes mimetes*) and the other, *A. swainsonii insulanus* Davison is transferred as a subspecies of *A. mimetes* (now *A. mimetes insulanus*); a species from Tasmania, the Tasman Peninsula Dusky Antechinus, is named *A. vandycki* sp. nov. These taxa are strongly differentiated: geographically (in allopatry), morphologically (in coat colour and craniodental features) and genetically (in mtDNA, 7.5-12.5% between species pairs).

❒ *Marsupialia, Dasyuridae, dasyurid, carnivorous marsupial, Antechinus swainsonii, mimetes, insulanus, vandycki, taxonomy, Tasmania, Tasman Peninsula.*

The first antechinus was discovered by Geoffroy more than 200 years ago (1803), but the genus was not formally erected for almost another 40 years (Macleay 1841), shortly following the description of two other species by Waterhouse (in 1838 and 1840). Later, there followed two further new species, named by Thomas (in 1904 and 1923). No other species was named under *Antechinus* until Van Dyck (1980). In the decades that followed Van Dyck's description, the advent of molecular techniques permitted resolution of numerous cryptic taxa across many organismal groups, including mammals. A range of genetic studies in the 1980s /1990s tested relationships among various families and genera of Australian mammals, including dasyurids (e.g. Armstrong *et al.* 1998; Baverstock *et al.* 1982; Krajewski *et al.* 1997) and this work prompted description of other antechinus species (Dickman *et al.* 1998, Van Dyck & Crowther 2000). Van Dyck (2002) then conducted a comprehensive morphological review of antechinus, recognising ten extant species: Swamp Antrechinus, *A. minimus* (Geoffroy); Yellow-footed Antechinus, *A. flavipes* (Waterhouse); Brown Antechinus, *A. stuartii* Macleay; Dusky Antechinus, *A. swainsonii* (Waterhouse); Fawn Antechinus, *A. bellus* (Thomas); Rusty Antechinus, *A. adustus* (Thomas); Atherton Antechinus, *A. godmani* (Thomas); Cinnamon Antechinus, *A. leo* Van Dyck; Agile Antechinus, *A. agilis* Dickman, Parnaby, Crowther & King and Subtropical Antechinus, *A. subtropicus* Van Dyck & Crowther.

In the past three years, prompted by Van Dyck's suspicions that further cryptic taxa lay unresolved within antechinus, our research group undertook a systematic and taxonomic revision of the extant members of the genus; several new species were described as a result (see Baker, Mutton & Hines 2013; Baker, Mutton, Hines & Van Dyck 2014; Baker, Mutton & Van Dyck 2012; Baker & Van Dyck 2012, 2013a, b). The discovery sequence ran as follows. First, Baker, Mutton & Van Dyck (2012) diagnosed an eleventh species, the Buff-Footed Antechinus *A. mysticus*, previously referred to the ubiquitous Yellow-footed Antechinus, *A. flavipes*. Then, in the process of investigating the distributional range of *A. mysticus* between south-east and mid-east Queensland, Baker, Mutton & Hines (2013) found a twelfth antechinus species, the Silver-headed Antechinus, *A. argentus*. At about the time of discovering *A. argentus*, we began to shift our focus within the genus to the Dusky Antechinus, *Antechinus swainsonii*. The thirteenth species of Antechinus, *A. arktos*, was duly raised after comparison of northern outlying Dusky Antechinus populations with other mainland *A. s. mimetes* (Baker, Mutton, Hines & Van Dyck 2014). But further investigation showed that *A. swainsonii* was even more complex and better resolution of this group is the aim of the present work.

Antechinus swainsonii was originally described by Waterhouse (1840) from a Tasmanian specimen held in the private collection of William Swainson and later acquired by the British Museum. About three years after the description, Waterhouse, deferring to the judgment of Gould, synonymised *A. swainsonii* with *A. minimus* (Geoffroy 1803); however, it was another three years before Waterhouse was able to examine the *A. minimus* holotype and re-establish *swainsonii*. Subsequently, Thomas (1924) described the subspecies *A. swainsonii mimetes* from the Guy Fawkes district, NSW. In a checklist of Australian mammals, Iredale and Troughton (1934) attributed the distribution 'Northern New South Wales' to *A. s. mimetes*, and 'Tasmania, Victoria' to *A. s. swainsonii*. In response, Wakefield & Warneke (1963) noted the absence of a geographical break in the mainland distribution of *A. swainsonii*, a lack of morphological distinction between the populations from northern New South Wales and Victoria, and minimal morphological variation between the Victorian and Tasmanian populations. They therefore proposed the trinomial *A. s. swainsonii* be applied only to representatives of the species from Tasmania. They maintained that Thomas' trinomial *A. s. mimetes* should apply to the entire mainland population. However, some 46 years before Iredale and Troughton had published their checklist, Thomas (1888) had also made reference to the Victorian occurrence of the species. And later, Thomas (1924) again noted the Victorian distribution of the nominate form in his description of *A. s. mimetes*. Evidently, the establishment of *A. s. mimetes* was intended to contrast with the Victorian population, not contain it. Wakefield and Warneke (1963) were duly obliged to demonstrate sufficient division between Tasmanian and Victorian populations to justify retention of the trinomial *A. s. mimetes*; they could not do so, but in any case chose not to sink the subspecies.

More recent works have addressed the distinctiveness of mainland and Tasmanian subspecies of *A. swainsonii* (Smith 1983; Davison 1986, 1991). Smith (1983) examined electrophoretic variation in *A. swainsonii* on either side of Bass Strait and concluded that given a mean genetic distance of 0.085 +- 0.015 the trans- Bassian populations of *A. swainsonii* warranted (at least) subspecific status. The sampling of *A. swainsonii* in Smith's study was limited to a couple of Tasmanian populations (Arthur River and Mt Wellington) and no sampling of the mainland population was included near Guy Fawkes (north-east New South Wales, the type locality for *A. swainsonii mimetes*), being limited instead to two sites in southern Victoria (Gembrook and East Gippsland) and one in the ACT/NSW (Brindabella Ranges). Nevertheless, Smith's early genetic work clearly pointed towards the Tasmanian *A. swainsonii* being distinctive from mainland Victoria *A. swainsonii*. Later, Davison (1991) named *A. s. insulanus* based on morphology alone, in recognition of the generally larger animals from the Grampians Range, western Victoria, when compared with other mainland *A. s. mimetes*.

With the aforementioned studies in mind, and after the northern mainland *A. swainsonii* (now *A. arktos*) was recently recognised as specifically distinct from mainland *A. s. mimetes*, the stage was set for a thorough taxonomic revision of *A. swainsonii* across its geographic range. Here, we report the results of this work. We provide detailed holotype descriptions of *A. vandycki* sp. nov., *Antechinus swainsonii* (Waterhouse 1840) and *Antechinus swainsonii mimetes* (Thomas 1924), none of which have been described in detail previously. For detailed holotype descriptions of the remaining two members of the Dusky Antechinus complex, *A. swainsonii insulanus* Davison 1991 and *A. arktos* Baker, Mutton, Hines and Van Dyck 2014, we direct the reader to Davison (1991) and Baker *et al.* (2014), respectively.

MATERIALS AND METHODS

Fig. 1 describes and depicts the 30 skull and dental, and 5 external measurements taken. Measurements were made using Mitutoyo CD-8CSX digital calipers. Age variation was minimised by using only animals which possessed fully erupted permanent P^3 teeth and thus deemed to be adult. Tooth nomenclature follows Archer (1974) and basicranial nomenclature follows Archer (1976). Colour nomenclature used in the holotype pelage description follows Ridgway (1912).

Measured variables are as follows (and see Fig. 1): **wt** = body weight (grams); **hb** = head-body length (mm) from tip of nose to mid-vent; **tv** = tail-vent length (mm) from mid-vent to tip of tail proper (excluding hair at tip); **hf** = hind foot length (mm) from behind heel to tip of longest extended toe (excluding claw); **e** = ear length (mm) from extended ear tip to notch at rear base of tragus; **APV** = maximum anterior palatal vacuity length; **BL** = basicranial skull length, excluding incisors; **Dent** = dentary length, excluding incisors; **IBW** = minimum width between auditory bullae; **IOW** = minimum width of interorbital constriction; **IPV** = minimum interpalatal vacuity distance; **M^{2}W** = maximum width of upper molar 2 measured diagonally from anterior lingual to posterior labial points; **NW** = width of nasals at the nasal / premaxilla /maxilla junction; **OBW** = basicranial width from outside right and left auditory bullae; **PPV** = maximum posterior palatal vacuity length; **R-LC^1** = skull width level with the posterior of upper canines; **R-LM^1** = skull width level with the junction of the first and second upper molars; **R-LM^{1}T** = maximum width between the ectolophs of the left and right first upper molars; **R-LM^2** = skull width level with the junction of the second and third upper molars; **R-LM^3** = skull width level with the junction of the third and fourth upper molars; **ZW** = maximum zygomatic width; **HT**

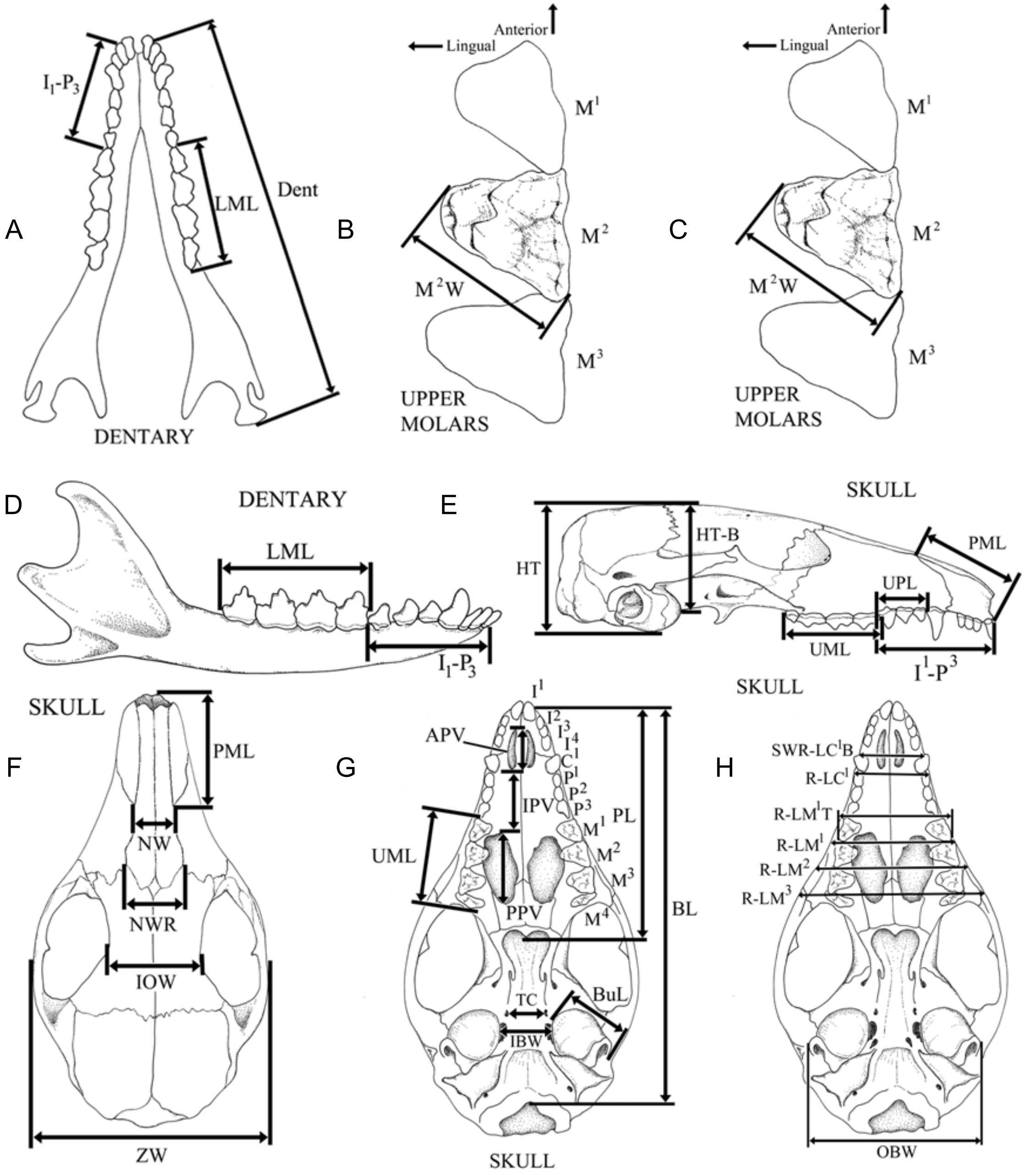

FIG. 1. Genus *Antechinus*; a guide to measurement of variables: skull and dentary (A-H).

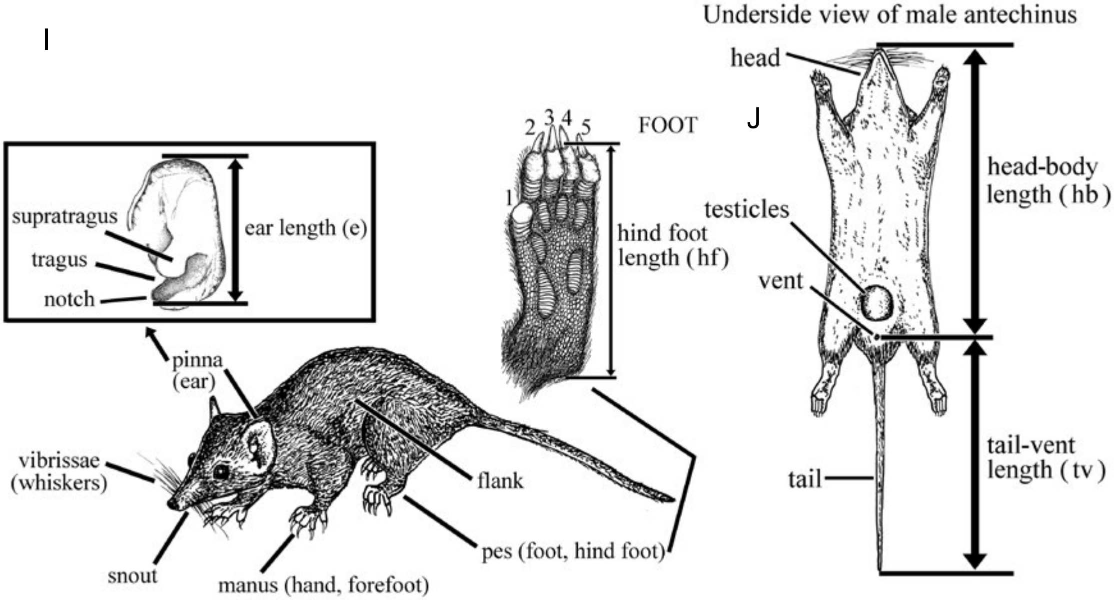

FIG. 1 continued. External body measures (I-J).

= skull height; **PL** = length of palate; **SWR-LC^{1}B** = skull width level with the anterior of upper canines; **TC** = minimum distance separating transverse canals; **NWR** = width of nasals at the nasal / maxilla / frontal junction; **PML** = length of premaxilla; **UML** = maximum length of upper molar row, M^1-M^4; **HT-B** = skull height measured immediately anterior of auditory bullae; **BuL** = auditory bulla length; **I^1-P^3** = crown length from anterior edge of upper incisor 1 to posterior edge of upper premolar 3; **LML** = maximum length of lower molar row, M$_1$-M$_4$; **I$_1$-P$_3$** = crown length from anterior of lower incisor 1 to posterior of lower premolar 3; **M$_2$W** = maximum width of lower molar 2 measured diagonally from anterior lingual to posterior labial points; **UPL** = crown length of upper premolar row, P^1-P^3.

Species clades returned from constructed DNA-based phylogenies (see below) were used as testable hypotheses in subsequent morphological analyses; thus, multivariate analyses enabled us to predict membership of individuals in hypothesised species groups based on a combination of skull morphology variables, whereas univariate ANOVAS (and subsequent post-hoc tests) for each variable enabled us to test for significant variation within each variable and determine which variables differed for comparisons of our putative new species with each species pair. The combination of univariate and multivariate analyses was essential to permit both fine-scale pairwise comparisons demonstrating species by species differences to facilitate best-practice species management and also broadscale comparisons among all species within the Dusky Antechinus complex, to best illustrate differences across all Antechinus measured variables.

Statistical analyses of morphometrics were undertaken using the program STATISTICA Version 7 (Statsoft Inc. 2004). Samples were initially tested for normality with the Kolmogorov-Smirnov and Lilliefors tests and homogeneity of sample variances using Levene's test. Analysis of Variance (ANOVA) was used to analyse variation in means among all putative antechinus species (from AMB's compiled museum and live specimen measurement data), tested under separate hypotheses for each measured external and cranial/dentition variable. In each ANOVA, post-hoc unequal N HSD tests (a modification of Tukey's HSD) were used to test pairwise differences (at $P < 0.05$) in external variables and cranial/dentition measures between *A. swainsonii* and each proposed congener, to compensate for potential Type 1 errors and since sample sizes differed between species. Multivariate analyses were conducted to optimise dimensionality of each variable set and maximise relationships between variable sets. Discriminant Function Analysis (DFA) was used to determine assignment reliability within proposed species groupings and subsequent Canonical Variate Analysis (CVA) generated independent functions that best discriminated between the putative species.

Univariate statistics (means, standard deviations, range minima and maxima) were compiled for each of the external and internal (cranial/dental) measures for the four species (and 5 taxa) within the Dusky Antechinus species complex: the Black-tailed Dusky Antechinus, *A. arktos*; the Mainland Dusky Antechinus *A. mimetes* (supporting two subspecies - *A. m. mimetes* and *A. m. insulanus*); the Tasmanian Dusky Antechinus *A. swainsonii*; and the Tasman Peninsula Dusky Antechinus, *A. vandycki* sp. nov. A range of scatterplots were constructed to show the main discriminating variable pairs among these species. All members of the Dusky Antechinus complex are strikingly different in both size and morphology to all congeners, so no other species were included for these comparisons. External body measures, while included in univariate analyses, were excluded from exploratory multivariate analyses because of missing data (numerous museum specimens included only skull material for the registered specimen) - this served to maximise the number of individuals of each species used in any given multivariate analysis. Antechinuses are known to be sexually dimorphic in size (Marlow 1961; Soderquist 1995; Williams & Williams 1982), so sexes were analysed separately for all measured variables. No *A. vandycki* sp. nov. female could be captured by us, so morphological analyses were conducted on males of that species only.

Analyses of Genetic Data. Comprehensive examination of genetic structuring in the genus *Antechinus* is the subject of an ongoing parallel research project and as such will not be presented in detail here. However, for the purpose of postulating DNA-based species groups that are subsequently tested with a comprehensive morphological data set, we present the preliminary DNA-based phylogenies for all recognised extant antechinus species, as well as DNA uncorrected percentage divergence ranges between each existing species paired with *A. swainsonii* (see results). A portion (607bp) of the mitochondrial Cytochrome B gene (CytB) and a portion (699bp) of the nuclear Interphotoreceptor Binding Protein gene (IRBP) were targeted using primers as described in Mutton (2011). Sequences were aligned by eye using Bioedit Version 7.1.11 (Hall 1999). Bayesian phylogenies (using mtDNA alone and also a concatenated dataset partitioned as mtDNA and nDNA) were reconstructed using MrBayes Version 3.2.1 (Ronquist & Huelsenbeck 2003), under the General Time Reversible Model of sequence evolution as determined by MrModelTest 2.3 (Nylander 2004), incorporating invariant sites and a gamma shape distribution of 2; in MrBayes, tree search was run for 10 million generations with a 25% burnin, as recommended by program guidelines. Resulting phylogenies were output in the program Treeview (Page 1996). A p-distance matrix was output based on aligned sequences in MEGA 6 (Tamura *et al.* 2013) and % divergences calculated by multiplying each value by 100; % divergence ranges incorporating mimima and maxima were generated for each putative species pair.

Abbreviations for museums housing material examined in this paper are: BMNH, Natural History Museum, London (formerly British Museum of Natural History); C, Museum Victoria, Melbourne; J and JM, Queensland Museum, Brisbane; and QVM, Queen Victoria Museum and Art Gallery, Launceston.

SYSTEMATICS

Antechinus vandycki sp. nov.
(Figs 17–18)

Etymology. Named in honour of Dr Steve Van Dyck, former Senior Curator of Mammals and Birds at the Queensland Museum, for his pioneering taxonomic work on the genus *Antechinus*.

Material examined. *Holotype*. Queensland Museum, Brisbane. JM20111, Male. Study skin and skull; remainder of body tissues in spirit (refer Figs 17-18). Captured on 7 May, 2014, by Eugene Mason, Emma Gray and Hannah Maloney in an Elliott trap (type A, Elliott Scientific), baited with peanut butter, rolled oats, peanut oil and bacon.

Paratypes. All paratypes were genetically typed and were either the same haplotype as the holotype or were characterised as a second haplotype that was only 2 bases different (0.4% divergent) to the holotype specimen. **Males**: JM 20113, JM 20116 Fortescue Road, Fortescue Bay, Tasman Peninsula, Tasmania 43°08′40″S, 147°57′18″E; JM 20114 Balt's Road, Tasman Peninsula, Tasmania 43°04′48″S, 147° 56′57″E; JM 20115, JM 20117 Lichen Road, Tasman Peninsula, Tasmania 43°03′07″S, 147°54′56″E.

Referred specimen. Male, BMNH 41.1246 Tasman's Peninsula, Tasmania.

Type Locality. Lichen Road, Tasman Peninsula, Tasmania, 43°03′07″S, 147°54′56″E, (refer Fig.19).

Habitat. Habitat of the type locality is wet sclerophyll temperate rainforest with many fallen logs and a dense understorey. Floristically, the area is typical of Tasmanian temperate rainforest, but there are only limited stands existent on Tasman Peninsula. The holotype locality featured Native Laurel, *Anopterus glandulosa*, with *Eucalyptus delegatensis* and *Eucalyptus obliqua* and an understorey of predominant *Blechnum nudum*.

Diagnosis. *Antechinus vandycki* sp. nov. differs from all other members of the *Antechinus swainsonii* complex in having longer anterior palatal vacuities, smaller inter-palatal vacuity distance and larger posterior palatal vacuities. *Antechinus vandycki* sp. nov. is most similar to *A. swainsonii*; both these species have predominantly greyish fur (although *A. vandycki* sp. nov. is darker), rather than the predominantly brownish *A. mimetes* and *A. arktos*. *Antechinus vandycki* sp. nov., like other Dusky Antechinus Complex species, is easily distinguished from other antechinus, being notably larger and longer/more narrow-snouted than most other species, except *A. minimus*, to which it differs markedly in coat colour and body shape (*A. vandycki* sp. nov. is greyish brown, longer tailed and less squat, whereas *A. minimus* is greyish merging to yellowish/brown with a markedly short tail and heavy hind-quarters).

Description. Holotype skin and skull are shown in Figs 17-18.

External Measurements. body weight – 89.1 g; hindfoot length – 24.6 mm; head-body length – 132.6 mm; tail-vent length – 118.0 mm; ear length – 16.7 mm.

Pelage. Colours for the *A. vandycki* sp. nov. holotype are as follows: fur of the mid-back, up to 17 mm long with basal 14 mm Deep Gull Gray, median 1 mm Dresden Brown and apical 1 mm Fuscous black. The back appears overall to be Prout's Brown on the flanks but is darker, Slate Black, on the upper back such that the animal appears to have a broad blackish-coloured back (enhanced by the dense fuscous guard hairs), merging gradually to Prout's Brown and even tinges of Dresden Brown on the flanks. Guard hairs (medially-thickened) are Fuscous black; they are prominent giving an overall moderately shaggy appearance, and up to 20 mm long on the rump, reducing to 6 mm where they terminate at the crown of the head. The crown of the head and upper snout are Slate Black with Prout's Brown highlights merging to greyish-Dresden Brown highlights on the cheeks and under the eye. The holotype lacks a head-stripe and eye patches although there are mottled Dresden Brown highlights both above and particularly below the eye. The soft ventral fur, up to 10 mm long on the belly is Deep Neutral Gray on the basal 6 mm and Pale Olive-Buff-Whitish on the apical 4 mm. It is interspersed by medially-thickened spines up to 16 mm long. Forefeet and hindfeet are darkish; Dark Olive on the upper and lower surface; the underside of both fore and hindfeet are covered in Dark Olive pigmented granules, which give it its overall darkish appearance. The claws on the forefoot are exceptionally long, up to 5.6mm, and slightly longer than the claws on the hindfoot (up to 4.0 mm). The tail is dark, Chaetura Black on the upper surface and similar in colour to the darkish guard hars on the rump; the tail is bicoloured, Chaetura Black on the dorsal surface with a lighter olive brown on the underside. The tail hairs are dense, fine and evenly moderate (6 mm). The overall impression of the animal is deep dark grey on the back, lighter dirty grey on the underside with brownish highlights on the body that are more notable on the flanks and also subtly towards the rump, with darkish brown-grey feet and a subtly bicoloured tail (dark grey on top and lighter brownish grey underneath).

Vibrissae. Approximately 20 mystaceal vibrissae occur on each side and these are up to 27 mm long. They are Fuscous Black in colour some merging to lighter browns and even to colourless at the tips. Supra-orbital vibrissae (Fuscous Black) number 1 on the right and 1 on the left; genals (Fuscous Black and colourless) number 4 right and 4 left; ulna-carpals (fuscous-colourless) number 2 left and 2 right; and submentals (basally fuscous with colourless tips) number 2.

Tail. The tail is shorter than the head and body. It is thick at the base (6.5 mm) and tapers gradually towards the tip.

Hindfoot. Interdigital pads are separate. The elongate hallucal and post-hallucal pads are separate on the right foot but connected on the left foot. The metatarsal pad is long and oval shaped; all the foot pads are heavily striate. Claws are very long (longest on hindfoot measures 4.0 mm; longest on forefoot measures 5.6 mm).

Ear. For a large antechinus (89.1g), the ears are smallish (16.7 mm); the supratragus is uncurled.

Dentition. Upper Incisors. All upper incisors are blade-like, procumbent. I^1 is broad, triangular, curved slightly anteriorly and uncurved posteriorly, two times taller-crowned than all other incisors and separated by a small (0.1 mm) diastema from I^2. The flaring crown of I^1, spreading posteriorly as well as anteriorly, does not quite meet the procumbent, flared I^2. Left and right I^1 broadly contact to form a cutting 'V'. In crown size I^3=I^2>I^4. I^2 and I^3 lack buccal cingula, but posterior buccal cingula are present on both I^4 and to a lesser extent I^1. There is no lack of differentiation between root and crown. All crowns are long antero-posteriorly, lower and rounded in I^2 and I^3, but higher and peaked in I^1 and I^4. I^4 and to a lesser extent I^1 carry a small posterior cusp.

Upper canines: C^1 is very slender and caniniform with a distinct anterior cusp but no posterior cusp. There is a very weak buccal cingulum and no lingual cingulum.

Upper premolars: All premolars are exceptionally narrow, slender and widely-spaced. Diastemata occur between C^1 and P^1 (0.6 mm), P^1 and P^2 (0.4 mm), P^2 and P^3 (0.3 mm), although P^3 contacts M^1. All premolars carry buccal and lingual cingula. In crown size: (right) P^3>P^2>P^1, (left) P^3>P^2>P^1. Minute anterior cingular cusps occur on P^{1-3}. Large posterior cusps occur on P^1, P^2 and P^3. No upper premolars possess posterolingual lobes, although there is a slight swelling in this area of P^2.

Upper molars: In M^1, the posterior tip of P^3 is positioned in the parastylar corner but lingual to and well below the minute stylar cusp A. The anterior cingulum below stylar cusp B is short, broad and incomplete. Stylar cusp B is moderately large, clearly peaked and about half the height of the paracone; there is no protoconule evident. Stylar cusps C and E are small, rounded peaks. M^1 lacks a posterior cingulum. The metacone is immediately lingual to, and larger than, stylar cusp D, the latter forming a large, rounded peak. The line from the metastylar corner of M^1 to the tip of the protocone is greatly indented and the post-protocrista is heavily swollen.

In M^2, the broad anterior cingulum which contacts the metastylar corner of M^1 tapers quickly as it progresses down and along the base of the pre-paracrista and finally degenerates before meeting the trigon basin. The protocone forms a rounded peak; no protoconule is evident. M^2 has low and indistinct stylar cusps A, B, C and E. Stylar cusp D forms a clear, rounded peak but is smaller than the metacone; there is no posterior cingulum.

In M^3, the anterior cingulum is broader and slightly longer than in M^2. It becomes indistinct after covering 2/3 distance between stylar cusp B and the lingual base of the paracone. There is no protoconule evident. Stylar cusps A, C and E are low and rounded. Stylar Cusp B is a low, rounded peak and stylar cusp D is a distinct peak but barely as high as the paracone and only 1/3 as high as the metacone.

In M^4, the ectoloph between stylar cusps B and D is greatly indented. The narrow anterior cingulum terminates gradually away from the anterior corner of M^4 and a posterior cingulum is absent. The protocone is greatly reduced and very narrow. In occlusal view, the angle made between the post-protocrista and the post-paracrista is close to 90°.

Lower incisors: All lower incisors project horizontally from the tip of the dentary. In crown height: I_1>I_2>I_3. I_3 is incisiform in lateral view with an inconspicuous posterior cusp at the base of the crest which descends posteriorly from the apex of the primary cusp. The lower canine rests against this posterior cusp. In occlusal view of I_3, a very small notch separates the posterior cusp from the prominent posterolingual lobe, and the crown enamel of the primary and posterior cusps fold lingually such that the crest of the two cusps bisects the tooth longitudinally.

Lower canines: C_1 is premolariform and long. There is mild anterior but minimal posterior curvature from root to crown tip and the tooth is short-crowned. It has weak buccal and lingual cingulation and a clear posterior cusp. The posterior edge of the tooth peak descends at a point that falls in the front half of the total tooth length; thus this tooth appears in buccal view to be strongly peaked at the front but low-slung and long before terminating in a clearly peaked posterior cusp.

Lower premolars: All premolars are extremely elongate and narrow. There are clear, narrow (0.1-0.2 mm) diastemata separating all premolars, and C_1-P_1 as well as P_3-M_1. In crown height: P_2>P_3>P_1. All premolars possess posterior cusps, which in P_1 and P_2 are very long. No premolars possess anterior cusps, except LP_1, where the cusp is minute. The bulk of premolar mass is concentrated anteriorly to the line drawn transversely through the middle of the two premolar roots. Postero-lingual lobes are not features of the lower premolars but a narrow cingula surrounds each tooth.

Lower molars: All molars are very narrow. In M_1, the talonid is wider than the trigonid and no anterior cingulum is present. A narrow, weak posterior cingulum extends from the hypoconulid around to the posterior base of the protoconid, with a very narrow posterior buccal shelf. The narrow paraconid appears in occlusal view as a small, steeply sided spur with an appreciable shelf. The paraconid makes little contribution to the bulk of the ectoloph enamel. The metacristid and hypocristid are oblique to the long axis of the dentary. The cristid obliqua is short, shallow and extends from the hypoconid to the posterior wall of the trigonid, intersecting the trigonid at a point slightly buccal to that point directly below the tip of the protoconid. The protoconid is large, about twice the height of the metaconid, which itself is twice the height of the low paraconid. The hypocristid terminates at the buccal base of the hypoconulid. The entoconid is a broad, low, rounded hump. From the base of the metaconid posteriorly, the talonid endoloph follows the line of the dentary until the base of the hypoconulid, allowing for a lingual bulge formed by the entoconid.

In M_2, the trigonid is about as wide as the talonid. The anterior cingulum is poorly yet distinctly developed, originating lingually in a weak parastylid notch into which the hypoconulid of M_1 is tucked. There is no buccal cingulum. A narrow, weak posterior cingulum extends from the hypoconulid to the posterior base of the hypoconid. The paraconid is well developed, but is the smallest trigonid cusp, with the metaconid slightly larger and protoconid clearly largest, and more than twice the height of the paraconid. The entoconid is a clearly, well-rounded peak, perhaps twice the height of the entoconid in M_1. A short cristid obliqua extends from the hypoconulid intersecting the posterior wall of the trigonid at a point directly below the tip of the protoconid, which is well buccal to the metacristid fissure. From the base of the metaconid posteriorly, the endoloph follows the line of the dentary axis, allowing for the distinctive lingual swelling of the entoconid.

In M_3, the trigonid is wider than the talonid. A very weak parastylid wraps around the hypoconulid of M_2, and the M_3 anterior cingulum is weak but clear. There is no buccal cingulum but the weak posterior cingulum is as in M_2, although even more poorly developed. The reduced cristid obliqua intersects the trigonid at a point slightly lingual to the tip of the protoconid, which is a great distance buccal to the metacristid fissure. A high, round-peaked entoconid is present, which is perhaps twice the height of the entoconid in M_2. The endoloph of the M_3 talonid takes a slightly more buccal orientation than that seen in M_2. The rest of M_3 morphology is as in M_2.

In M_4, the trigonid is much wider than the talonid. The anterior cingulum is as in M_3 but the posterior cingulum is absent. A narrow buccal cingulum occurs between the trigonid and the talonid. Of the three main trigonid cusps, the metaconid is about 1.5 times taller than the paraconid but both are markedly smaller than the protoconid, the latter being about twice the height of the paraconid. The cristid obliqua forms a low, weak crest which contacts the trigonid wall slightly lingual to the metacristid fissure. Of the talonid cusps, the small, rounded hump of the entoconid is the largest cusp. The hypoconid is very weakly formed, while the hypoconulid is a rounded nubbin and all but absent.

Skull. The holotype skull is intact, in excellent condition, with only nominal tooth wear. The skull is characterised by a very long, narrow, low, rostrum which is tubular in cross section. The nasals are very narrow anteriorly and flare noticeably, posteriorly. Anteriorly the nasals are set well back from the inclined anterior edge of the premaxillaries. Slight flattening of the skull only occurs at the junction of the nasals and frontals, and the cranium is high and domed. The exceptionally large (7.16 mm) premaxillary vacuities extend from the level of the posterior of the I^2 root back to slightly posterior of the posterior of the P^2 root. The maxillary vacuities are also exceptionally large (6.54 mm), extending from slightly anterior to the level of the protocone root of M^1 back to the posterior of the protocone root of M^4.

Comments. We recommend the following common name be used in association with *A. vandycki* sp. nov.: Tasman Peninsula Dusky Antechinus.

Antechinus swainsonii (Waterhouse, 1840)

Phascogale swainsonii Waterhouse, 1840
Antechinus rolandensis Higgins and Petterd, 1882
?*Antechinus niger* Higgins and Petterd, 1883
?*Antechinus moorei* Higgins and Petterd, 1884
?*Antechinus moorei* var. *assimilis* Higgins and Petterd, 1884

Material examined. *Holotype*. BMNH 60.1.5.18 (skin) and 60.1.5.26 (skull) (male) from the private collection of William Swainson, given to Waterhouse.

Other material. These specimens were formalin-fixed and old, so genetic analysis was not possible. Only adults were used for morphometrics and specimens were selected to be representative of the species' geographic range. **Males**: JM 20107 Mt Field NP off Lake Dobson Road, Tasmania 42° 41´S 146° 39´E; BMNH 87.5.18.10 Table Cape, Tasmania; BMNH 4.6.26.11 Magnet, Tasmania; QVM 1959:1:0012 Fingal, Tasmania; QVM 1963:1:0089 Mount Kate, Tasmania; QVM 1963:1:0189 Waratah, Corinna Rd, Tasmania; QVM 1965:1:0109 Renison Bell, Tasmania; QVM 1981:1:0152, QVM 1982:1:0136, QVM 1985:1:0005, QVM 1985:1:0006 Mount Barrow, Tasmania; QVM 1984:1:0116 Mount Arthur, Tasmania. **Females**: JM 4381 Button grass plains, eagle creek track, south-west Tasmania; QVM 1982:1:0133 Mount Barrow, Tasmania; QVM 1984:1:0143 Mount Arthur, Tasmania; QVM 1985:1:0016 Mount Barrow, Tasmania; QVM 1963:1:0043 between Erriba and Cradle Mountain, Tasmania; QVM1963:1:0087 Mount Kate, Tasmania; QVM 1963:1:0187 Waratah, Corinna Road, Tasmania; QVM 1964:1:0042 Renison Bell, Tasmania; QVM 1964:1:0094 Mount Kate, Tasmania.

Type Locality. Van Diemen's Land, Tasmania.

Rediagnosis. *Antechinus swainsonii sens. strict.* differs from all other members of the Dusky Antechinus complex in having the slenderest-looking snout. *Antechinus swainsonii* is most similar to *A.vandycki* sp. nov. but has shorter anterior palatal vacuities, larger inter-palatal vacuity distance and smaller posterior palatal vacutiies; both species are greyish-brown in appearance, moderate-dark grey on the back, pale grey on the sides and light grey-white on the underside with brownish highlights on the body that are more notable on the flanks and also with brownish warming towards the rump. The tail in both species is bicoloured. However, *A. swainsonii* is distinctly paler in overall appearance than *A. vandycki* sp. nov. Both *A. swainsonii* and *A. vandycki* sp. nov. have predominantly greyish fur, rather than the predominantly brownish *A. mimetes* and *A. arktos. Antechinus swainsonii*, like other Dusky Antechinus complex species, is easily distinguished from other antechinus, being notably larger, shaggier and longer/ more narrow-snouted than most other species, except *A. minimus*, to which it differs markedly in coat colour and body shape (*A. swainsonii* is greyish brown, longer tailed and less squat, whereas *A. minimus* is greyish merging to yellowish/ brown with a markedly short tail and heavy hind-quarters). For individual species-pair comparisons of *A. swainsonii* to all congeners, refer to the species by species section in Results.

Description. Holotype, skin and skull are shown in Figs 13-14.

Pelage. Colours for the holotype are as follows: fur of the mid-back, up to 12.5 mm long with basal 10.5 mm Slate Colour, median 1 mm Prouts Brown and apical 1.0 mm Fuscous black. The back appears overall to be Chestnut Brown. Guard hairs (medially-thickened) are Fuscous black fading to Sepia. They are up to 20 mm long on the rump and reduce to 6 mm where they terminate at the crown of the head. Fur on, and below the shoulders, thighs, flanks and chin, lacks black tips and these areas appear as Deep Olive Gray. The tips of the guard hairs warm to a more rufous shade toward the rump.

The holotype lacks a head-stripe and there is no eye-ring present. The soft ventral fur, up to 10 mm long on the belly is Dark Mouse Gray on the basal 8.5 mm and Pale Smoke Grey on the apical 1.5 mm. It is interspersed by medially-thickened spines 11 mm long. The belly is thus an overall Deep Olive Gray. Forefeet are thinly covered with Bister coloured hairs and hindfeet are more thickly covered with darker Sepia-coloured hairs. The tail is weakly bicoloured with hairs averaging 3 mm along its length and increasing to 4 mm at its tip. Dorsally, the tail-hairs are a uniform Clove Brown. Ventrally they are Olive Brown.

Vibrissae. Approximately 24 mystaceal vibrissae occur on each side and are up to 16 mm long (many, however, are broken). All are Fuscous Black. Supra-orbital vibrissae (Fuscous Black) number 6 right and those on the left have been cut off; genals (Fuscous Black and colourless) number 6 right but those on the left cannot be seen; ulna-carpals (colourless) number 5 left and 1 right; and submentals (all cut) number 4.

Tail. The tail is shorter than the head and body. It is thin and tapers towards the tip.

Hindfoot. Interdigital pads are separate. The apical granule is enlarged, elongate and striate. The enlarged hallucal and post-hallucal pads are fused. Metatarsal pads are not visible in the holotype. Claws are very long.

Ear. On the holotype the pinnae are not present.

Dentition. Upper Incisors. All upper incisors are procumbent and badly worn. I^1 is broad, triangular and uncurved, two times taller-crowned than all other incisors and is not separated by a diastema from I^2. The flaring crown of I^1, spreading posteriorly as well as anteriorly, meets the procumbent, flared I^2 so that the natural diastema between I^1 and I^2 is filled. Left and right I^1 contact to form a cutting 'V'. In crown size: $I^3=I^2>I^4$ (but they are all badly worn). All upper incisors, but for I^4, lack buccal cingula and in I^4 the cingula is positioned to the posterior of the tooth. There is no lack of differentiation between root and crown. All crowns are long antero-posteriorly and low. I^4 carries no anterior or posterior cusp. The roots of I^4 are wide.

Upper canines: C^1 is very slender and caniniform with an indistinct boundary between the root and crown. There is a very weak buccal cingulum and no lingual cingulum. No anterior cusp is present but there is a minute posterior cusp.

Upper premolars: All premolars are exceptionally narrow and slender. Diastemata occur between C^1 and P^1, P^1 and P^2 (diastemata equally sized at 0.5 mm), P^2 contacts P^3 and P^3 contacts M^1. All premolars carry very weak buccal and weak lingual cingula. In crown size: (right) $P^2>P^3>P^1$; (left) $P^3=P^2>P^1$. Minute anterior cingular cusps occur on P^{1-3}. Large posterior cusps occur on P^2 and P^3. No upper premolars possess posterolingual lobes.

Upper molars (note that LM^{2-4} are missing): The posterior tip of P^3 is positioned in the parastylar corner of M^1 but lingual to and well below the minute stylar cusp A. The anterior cingulum below stylar cusp B is short, broad and incomplete. Stylar cusp B is moderately large but the paracone is worn down to a nubbin and there is no protoconule present. Stylar cusps C and E are not present. M^1 lacks a posterior cingulum. The metacone is immediately lingual to, and larger than, stylar cusp D. The line from the metastylar corner of M^1 to the tip of the protocone is greatly indented and the post-protocrista is heavily swollen.

In RM^2, the broad (worn) anterior cingulum which contacts the metastylar corner of M^1 tapers quickly as it progresses down and along the base of the pre-paracrista; it finally degenerates before meeting the trigon basin. The protocone is badly worn and no protoconule is present. M^2 lacks stylar cusps A, C and E. Stylar cusp D is greatly reduced and smaller than the metacone and there is no posterior cingulum. LM^2 is missing.

In RM^3, the worn anterior cingulum is broader and slightly longer than in RM^2. It becomes indistinct after covering 2/3 distance between stylar cusp B and the lingual base of the paracone. There is no protoconule. Stylar cusp D is reduced to a small, rounded peak, which is about half the height of the metacone. Stylar cusp C is absent and E is a worn rudament.LM^3 is missing.

In RM^4, the ectoloph between stylar cusps B and D is greatly indented. The narrow anterior cingulum terminates quickly away from the anterior corner of M^4 and a posterior cingulum is absent. The protocone is greatly reduced and very narrow. In occlusal view, the angle made between the post-protocrista and the post-paracrista is close to 90°. LM^4 is missing.

Lower incisors: All lower incisors are heavily worn and project horizontally from the tip of the dentary. In crown height: $I_1>I_3>I_2$. I_3 is incisiform in lateral view with an inconspicuous posterior cusp at the base of the crest which descends posteriorly from the apex of the primary cusp. The lower canine rests against this posterior cusp. In occlusal view, a very small notch separates the posterior cusp from the prominent posterolingual lobe, and the crown enamel of the primary and posterior cusps fold lingually such that the crest of the two cusps bisects the tooth longitudinally.

Lower canines: The RC_1 is broken off at the root. LC_1 is premolariform and is characterised by excessive thegotic wear of the lower posterior surface. There is minimal curvature from root to crown tip and the tooth is short-crowned. It has weak buccal and lingual cingulation and a weak posterior cusp.

Lower premolars: All premolars are extremely elongate and narrow. There are no diastemata separating premolars, and contact is made between adjacent teeth from C_1 to P_3; however, there is a minute diastema between P_3 and M_1. Although there is contact between lower premolars, there is no crushing. In crown height: $P_2>P_3>P_1$. All premolars possess weak posterior cusps, which in P_1 and P_2 are very long. No premolars possess anterior cusps. The bulk of premolar mass is concentrated anteriorly to the line drawn transversely through the middle of the two premolar roots. Postero-lingual lobes are not features of the lower premolars but a narrow cingula surrounds each tooth.

Lower molars: All molars are very narrow and heavily worn. In M_1 the talonid is wider than the trigonid and no anterior cingulum is present. A narrow, weak posterior cingulum extends from the hypoconulid to the posterior base of the protoconid, with a very narrow posterior buccal shelf. The very narrow paraconid appears in occlusal view as a small, steeply sided spur with an appreciable shelf. The paraconid makes little contribution to the bulk of the ectoloph enamel. The badly worn metacristid and hypocristid are oblique to the long axis of the dentary. The cristid obliqua is short and shallow and extends from the hypoconid to the posterior wall of the trigonid intersecting the trigonid at a point probably slightly lingual to that point directly below the tip of the protoconid. However, the posterior half of the protoconid is worn away so it is difficult to be precise. The hypocristid terminates at the buccal base of the hypoconulid. The entoconid is a rounded rudiment. From the base of the metaconid posteriorly, the talonid endoloph follows the line of the dentary until the base of the hypoconulid.

In M_2, the trigonid is slightly wider than the talonid. The anterior cingulum is very poorly developed originating lingually in a weak parastylid notch into which the hypoconulid of M_1 is tucked. There is no buccal cingulum. A narrow, weak posterior cingulum extends from the hypoconulid to the posterior base of the hypoconid. The paraconid is well developed, but is the smallest trigonid cusp, with the metaconid larger and protoconid largest. However, the protoconid is poorly developed (likely due to wear) relative to the other lower molars M_3 and M_4, and low crowned, while the metaconid is partly worn. The entoconid is poorly developed. A short cristid obliqua extends from the hypoconulid intersecting the posterior wall of the trigonid at a point directly below the tip of the protoconid, which is well buccal to the metacristid fissure. From the base of the metaconid posteriorly, the endoloph follows the line of the dentary axis.

In M_3, the trigonid is wider than the talonid. A very weak parastylid wraps around the hypoconulid of M_2, and the M_3 anterior cingulum is very weak. There is no buccal cingulum but the weak posterior cingulum is as in M_2 but more poorly developed. The reduced cristid obliqua intersects the trigonid at a point directly below the tip of the protoconid, which is a great distance buccal to the metacristid fissure. A low, rounded entoconid is present. The endoloph of the M_3 talonid takes a slightly more buccal orientation than that seen in M_2. The rest of M_3 morphology is as in M_2.

In M_4, the trigonid is much wider than the talonid. The anterior cingulum is as in M_2 but the posterior cingulum is absent. A small buccal cingulum occurs between the trigonid and the talonid. Of the three main trigonid cusps the metaconid is slightly taller than the paraconid but both are markedly smaller than the protoconid. The cristid obliqua forms a low, weak crest which contacts the trigonid wall slightly lingual to the metacristid fissure. Of the talonid cusps, the small entoconid is the largest cusp. The hypoconid is very weakly formed but the hypoconulid is absent.

Skull. The holotype skull is characterised by a long, narrow, low, rostrum which is tubular in cross section. The nasals are very narrow anteriorly and flare noticibly posteriorly. Anteriorly, the nasals are set well back from the inclined anterior edge of the premaxillaries. Slight flattening of the skull only occurs at the junction of the nasals and frontals, and the cranium is high and domed. The large premaxillary vacuities extend from the level of the I^2 root back to the level of the middle of the P^2 root. The maxillary vacuities extend from the level of the protocone root of M^1 but all the palate is broken and smashed beyond this.

Comments. We recommend the following common name to be used in association with *A. swainsonii*: Tasmanian Dusky Antechinus.

There are several synonyms for *A. swainsonii*. First is *Antechinus rolandensis* Higgins and Petterd, 1882, based on a male, no registration number from Mount Roland (about 60 km west of Launceston), Tasmania. This species was initially assigned to synonymy with *A. minimus* (Thomas, 1888; Iredale and Troughton, 1934; Tate, 1947; Wakefield and Warneke, 1963; Mahoney and Ride, 1988 (who corrected the publication date from 1883 to 1882, probably on the authority of Thomas (1888) who nevertheless gives no indication that he examined the specimen)). However, Van Dyck (1997, 2002) noted measurements provided by the authors placed it as a very large animal and thus was most likely *A. swainsonii*. We concur with

Van Dyck's assessment. There are three other synonyms of *A. swainsonii* from elsewhere in Tasmania. First, *Antechinus niger* Higgins and Petterd (1883: 172), based on a female (no registration number) from (presumably) Upper Piper (now Lilydale, 28 km north-east of Launceston), Tasmania. Second, *Antechinus moorei* Higgins and Petterd (1884: 182), based on a male (no registration number) from Long Plains (north of Launceston), Tasmania. Third, *Antechinus moorei* var. *assimilis* Higgins and Petterd (1884: 185), based on a specimen (sex unstated, 'in the museum of the Royal Society, Hobart') from 'Tasmania, West Coast. Thomas (1888), Iredale and Troughton (1934), Tate (1947) and Wakefield and Warneke (1963) all assign these three novelties to the synonymy of *A. swainsonii*.

And yet, all four type specimens noted above have never featured in the literature (as they are presumed lost), the descriptions are too inadequate to enable an accurate determination, and there is no indication that Thomas (1888) ever saw them. In their comprehensive review of the time, Wakefield and Warneke (1963) could not find any of the specimens and presumed them lost. Subsequently, Van Dyck (1997, 2002), who also could not locate the specimens, thereby classed these species and subspecies *incertae sedis*; we concur with Van Dyck's assessment and would add this note regarding their probable identity: three locations are near Launceston in the north of Tasmania, and the other in western Tasmania. Thus, based on distribution alone, the synonyms, if they indeed still exist, are highly likely to be *A. swainsonii*, since *A. swainsonii* are known from locations nearby and encompassing the regions where the mystery types are found and also *A. vandycki* sp. nov. is apparently limited to Tasman Peninsula, far to the south-east. While on the subject of type localities and identities, it is worth noting that the *A. swainsonii* holotype specimen unfortunately has a vague locality descriptor of 'Van Diemen's Land'. A thorough search by AMB of the BMNH archives in July 2013 found a log book of William Swainson covering his visit to Australia in the mid-1800s but there was no mention of him acquiring *A. swainsonii*; thus, the generic type locality must stand. Measurements of this type specimen (BMNH 60.1.5.18 skin; BMNH 60.1.5.26 skull) indicate it is clearly *A. swainsonii* and not *A. vandycki* sp. nov. (based on APV and IPV, and several other craniodental measures). Furthermore, another specimen from the general collection held at the BMNH (41.1246) from 'Tasman's Peninsula, Tasmania' clearly clades out as *A. vandycki* sp. nov. rather than *A. swainsonii* (see species by species accounts and tables and figs therein).

Antechinus mimetes mimetes
(Thomas 1924) **new status**

Phascogale swainsonii mimetes Thomas, 1924

Rediagnosis of nominate form. *Antechinus mimetes mimetes* differs from all other members of the Dusky Antechinus complex in having shorter anterior palatal vacuities than *A. vandycki* sp. nov. and *A. swainsonii*, but longer anterior palatal vacuities than *A. arktos*. *Antechinus mimetes mimetes* differs from both *A. vandycki* sp. nov. and *A. swainsonii* in being predominantly brownish on head and shoulders, rather than greyish. *Antechinus mimetes mimetes* is most similar to *A. mimetes insulanus*, but differ in that the latter has a generally broader skull, particularly at the base of the snout. *Antechinus mimetes mimetes* differs from *A. arktos* in being more evenly brownish from head to rump with a brownish tail and hind feet, whereas *A. arktos* has more colourful orange-tonings on the rump and both a black tail and hind feet. *Antechinus mimetes mimetes*, like other Dusky Antechinus complex species, is easily distinguished from other antechinus, being notably larger and longer/more narrow-snouted than most other species, except *A. minimus*, to which it differs markedly in coat colour and body shape (*A. mimetes mimetes* is brownish, longer tailed and less squat, whereas *A. minimus* is greyish merging to yellowish/brown with a markedly short tail and heavy hind-quarters).

Material examined. *Holotype*. BMNH 24.10.1.1 (skin and skull), female, collected by Captain G.H. Wilkins on 14 April, 1924.

Other material. These specimens were formalin-fixed and old, so genetic analysis was not possible. Only adults were used for morphometrics and specimens were selected to be representative of the species' geographic range. **Males**: J 3809 Ebor, Guy Fawkes District, north-east NSW, 30° 24´S 152°21´E; JM 20012 Weeping Rock Walking Track, New England NP, NSW 30° 29´S 152° 24´E; BMNH 24.10.1.2 Guy Fawkes District, NSW 30° 30´S 152°30´E; BMNH 86.5.15.7 Gippsland; C 875 Beech Forest, Victoria 38°38´S 143°34´E; C 9671 Kentbruck, Victoria 38° 10´S 141° 17´E; C 9725 Little Moleside Creek, Victoria 38° 07´S 141° 19´E; C 13574 14.4 km west of Noojee, Victoria 37°54´S 145°50´E, C 13725 Allambee, Victoria 38° 16´S 146° 02´E; C 13738 Cumberland picnic ground, Victoria 37° 33´S 148° 51´E; C 13759 Loch Valley, Victoria 37°49´S 146°01´E; C 15933 Pomonal, Victoria 37° 12´S 142° 37´E; C 7047 Neerim Junction, Victoria 37° 56´S 145° 58´E; C 28737 Orbost Region, Victoria 37°26´S 148° 37´E. **Females**: JM 20011 Cliff's Trail New England NP, NSW 30°31´S 152° 23´E; JM 20112 The Chalet, off Point Lookout Rd, New England NP, NSW 30° 30´S 152°24´E; C 426, C 427 Hordam Vale, Victoria 38°46´S 143°30´E; C 2584 Eyre Plantation, Beech Forest, Victoria 38° 38´S 143° 34´E; C 7432 Wyelangta, Arkin's Catchment, Victoria 38°40´S 143°26´E; C 7715 Gellibrand River, Victoria 38°31´S 143°33´E; C 9687 Belgrave area, Victoria 37°55´S 145°21´E; C 13570, C 13794 Loch Valley, Victoria 37°49´S 146°01´E; C 13740 Noorinbee North, Victoria 37°26´S 149°12´E; C 24892 Sherbrooke Forest, Victoria 37°01´S 147°07´E.

Type Locality. Guy Fawkes District, via Ebor, north-east New South Wales, 30°30´S 152°30´E.

Description. *Antechinus swainsonii mimetes* Holotype skin and skull are shown in Figs 15-16.

Pelage. Colours for the holotype are as follows: fur of the mid-back, up to 12.5 mm long with basal 10.5 mm Slate-Gray, median 1 mm Prouts Brown and apical 1 mm Fuscous black. The back appears overall to be Mummy Brown tending towards a Sepia colour on the rump. Guard hairs (medially-thickened) are Fuscous black fading to Sepia. They are up to 20 mm long on the rump and reduce to 6 mm where they terminate at the crown of the head. Fur on, and below the shoulders, thighs, flanks and chin, lacks black tips and these areas appear as Deep Olive Gray. The tips of the guard hairs warm to a more rufous shade toward the rump. The holotype lacks a head-stripe and there is no eye-ring present, although the fur around the eye (particularly under it) and to a lesser extent between the eyes appears as Dresden Brown, as opposed to the generally Mummy Brown between the ears. The soft ventral fur, up to 10 mm long on the belly is Dark Mouse Gray on the basal 8.5 mm and Pale Smoke Grey on the apical 1.5 mm. It is interspersed by medially-thickened spines 11 mm long. The belly thus appears an overall Deep Olive Gray. Forefeet are thinly covered with Bister coloured hairs and hindfeet are more thickly covered with darker Sepia-coloured hairs. The tail is weakly bicoloured with hairs averaging 3 mm along its length and increasing to 4 mm at its tip. Dorsally, the tail-hairs are a uniform Clove Brown; ventrally, they are Buffy Brown.

Vibrissae. Approximately 24 mystaceal vibrissae occur on each side and are up to 16 mm long (many, however, are broken). All are Fuscous Black. Supra-orbital vibrissae (Fuscous Black) number 6 right and those on the left have been cut off; genals (Fuscous Black and colourless) number 6 right but those on the left cannot be seen; ulna-carpals (colourless) number 5 left and 1 right; and submentals (all cut) number 4.

Tail. The tail is shorter than the head and body. It is thin and tapers towards the tip.

Hindfoot. Interdigital pads are separate. The elongate hallucal and post-hallucal pads are fused on the left hindfoot and separate on the right hindfoot. The metatarsal pad is long and oval shaped; all the foot pads are heavily striate. Claws are very long (longest on hindfoot measures 3.1 mm; longest on front foot measures 4.3 mm).

Ear. The ears appear to be smallish and the supratragus is uncurled.

Dentition. Upper Incisors. All upper incisors are procumbent. I^1 is broad, triangular with a curved anterior plane, two times taller-crowned than all other incisors and is not separated by a diastema from I^2. The flaring crown of I^1, spreading posteriorly as well as anteriorly, meets the slightly procumbent, flared I^2 so that the natural diastema between I^1 and I^2 is filled. Left and right I^1 contact to form a cutting

'V', although RI^1 is worn at the tip. In crown size: $I^3>I^2>I^4$. All upper incisors, but for I^4, lack buccal cingula and in I^4 the cingulum is positioned to the posterior of the tooth. There is no lack of differentiation between root and crown. All crowns are long antero-posteriorly and low. I^4 carries no anterior or posterior cusp. The roots of I^4 are wide.

Upper canines: C^1 is very slender and caniniform with an indistinct boundary between the root and crown. There is a very weak buccal cingulum and no lingual cingulum. No anterior cusp is present but there is a minute posterior cusp.

Upper premolars: All premolars are exceptionally narrow and slender. Diastemata occur between C^1 and P^1, P^1 and P^2 (diastemata equally sized at 0.3 mm), P^2 contacts P^3 and P^3 contacts M^1. All premolars carry very weak buccal and lingual cingula. In crown size, (right): $P^3>P^2>P^1$; (left): $P^3>P^2>P^1$. Minute anterior cingular cusps occur on $P^{1\text{-}3}$. Large posterior cusps occur on $P^{1\text{-}3}$. No upper premolars possess posterolingual lobes.

Upper molars: The posterior tip of P^3 is positioned in the parastylar corner of M^1 but lingual to and slightly below the minute stylar cusp A. The anterior cingulum below stylar cusp B is short, broad and incomplete. Stylar cusp B is moderately large but smaller than the paracone and there is a small, rounded protoconule present; the paracone is smaller than stylar cusp D, which in turn is smaller than the metacone. Stylar cusp C is a worn rudiment and stylar cusp E is not present. M^1 possesses a weak posterior cingulum formed at the base of the post-protocrista and tapering posteriorly to a point level with the base of the post-metacrista; thus the protocone appears notably broad. The metacone is immediately lingual to, and larger than, stylar cusp D. The line from the metastylar corner of M^1 to the tip of the protocone is greatly indented and the post-protocrista is very heavily swollen.

In M^2, the very broad anterior cingulum which contacts the metastylar corner of M^1 tapers quickly as it progresses down and along the base of the pre-paracrista and finally degenerates before meeting the trigon basin. Stylar cusp B is smaller than stylar cusp D, which is slightly smaller than the paracone, which in turn in much smaller than the metacone; the protocone is well defined and about the same height as in M^1; there is a small, rounded protoconule present. M^2 lacks stylar cusp A, but stylar cusp E is a rounded rudiment and stylar cusp C is present, small and rounded. M^2 possesses a weak posterior cingulum formed at the base of the post-protocrista and tapering posteriorly to a point level with the base of the post-metacrista; thus the protocone appears notably broad.

In M^3, the anterior cingulum is subequal in breadth and slightly longer than in M^2. It becomes indistinct after covering 3/4 of the distance between stylar cusp B and the lingual base of the paracone. There is a small, rounded protoconule. There is no stylar cusp A; stylar cusp B and D form subequal, small but distinct peaks, which are smaller than the paracone, which in turn is smaller than the metacone; stylar cusp C is very small and stylar cusp E is absent. M^3 possesses a very weak posterior cingulum formed at the base of the post-protocrista and tapering posteriorly to a point level with the base of the post-metacrista; thus the protocone appears notably broad.

In M^4, the ectoloph between stylar cusps B and D is fairly straight. The narrow anterior cingulum tapers, forming a very narrow shelf that continues all the way to the base of the pre-protocrista; a posterior cingulum is absent. The protocone is greatly reduced and very narrow. In occlusal view, the angle made between the post-protocrista and the post-paracrista is about 50°.

Lower incisors: All lower incisors project horizontally from the tip of the dentary. In crown height: $I_1>I_2>I_3$. I_3 is incisiform in lateral view with a distinct posterior cusp at the base of the crest which descends posteriorly from the apex of the primary cusp. The lower canine rests against this posterior cusp. In occlusal view, I_3 has a very small notch separating the posterior cusp from the prominent postero-lingual lobe, and the crown enamel of the primary and posterior cusps fold lingually such that the crest of the two cusps bisects the tooth longitudinally. I_3 has a weak posterior buccal cingulum.

Lower canines: C_1 is premolariform. There is moderate curvature from root to crown tip and the tooth is short-crowned, only slighty larger than P_2. C_1 has weak buccal and lingual cingulation and a weak posterior cusp.

Lower premolars: All premolars are extremely elongate and narrow and there are clear diastemata separating all premolars from adjacent teeth. In crown height: $P_2 > P_3 > P_1$, such that P_2 is about 1.5 times the height of P_3 and about twice the height of P_1. All premolars possess distinct posterior cusps, which in P_2 is very long. No premolars possess anterior cusps. The bulk of premolar mass is concentrated anteriorly to the line drawn transversely through the middle of the two premolar roots. Postero-lingual lobes are not features of the lower premolars but a narrow cingulum surrounds each tooth.

Lower molars: All molars are very narrow. In M_1, the talonid is wider than the trigonid and no anterior cingulum is present. A narrow, weak posterior cingulum extends from the hypoconulid to the posterior base of the protoconid, with a very narrow posterior buccal shelf. The very narrow paraconid appears in occlusal view as a small, steeply sided spur with an appreciable shelf. The paraconid makes little contribution to the bulk of the ectoloph enamel. The metacristid and hypocristid are oblique to the long axis of the dentary. The cristid obliqua is moderate, about 45° and extends from the hypoconid to the posterior wall of the trigonid intersecting the trigonid at a point buccal to that point directly below the tip of the protoconid. The hypocristid terminates at the buccal base of the hypoconulid. The entoconid is low and rounded. From the base of the small peaked metaconid posteriorly, the talonid endoloph roughly follows the line of the dentary until the base of the hypoconulid although there is a slight lingual bulge.

In M_2, the trigonid is very slightly wider than the talonid. The anterior cingulum is narrow, originating lingually in a weak parastylid notch into which the hypoconulid of M_1 is tucked. A small buccal cingulum occurs between the trigonid and the taloned; a narrow, weak posterior cingulum extends from the hypoconulid to the posterior base of the hypoconid. The paraconid is well developed, but is the smallest trigonid cusp, with the metaconid larger and protoconid largest. However, the protoconid is well developed and subequal with protoconids on M_3 and M_4. The entoconid is a small but well-developed peak. A fairly steep (60°) cristid obliqua extends from the hypoconulid intersecting the posterior wall of the trigonid at a point directly below the tip of the protoconid, which is well buccal to the metacristid fissure. From the base of the metaconid posteriorly, the endoloph roughly follows the line of the dentary axis with a slight lingual bulge due to the entoconid swelling.

In M_3, the trigonid is wider than the talonid. A very weak parastylid wraps around the hypoconulid of M_2, and the M_3 anterior cingulum is moderate. A small buccal cingulum occurs between the trigonid and the taloned; the weak posterior cingulum is as in M_2. The fairly steep (60°) cristid obliqua intersects the trigonid at a point directly below the tip of the protoconid, which is well buccal to the metacristid fissure. The entoconid is a moderate,well-developed peak. From the base of the well-developed metaconid posteriorly, the endoloph of the M_3 talonid takes a slightly more buccal orientation than that seen in M_2.

In M_4, the trigonid is much wider than the talonid. The anterior cingulum is moderate but the posterior cingulum is absent. A small buccal cingulum occurs between the trigonid and the talonid. Of the three main trigonid cusps the metaconid is slightly taller than the paraconid but both are markedly smaller than the protoconid. The cristid obliqua forms a shallower (30 °), smaller crest which contacts the trigonid wall slightly buccal to the metacristid fissure. Of the talonid cusps, the small hypoconid is the largest cusp. The hypoconulid is more weakly formed and the entoconid is absent.

Skull. The left and right alisphenoid tympanic bullae are widely separated and only moderately enlarged. The foramen pseudovale is large as is the eustachian canal opening. The internal jugular canal foramina are moderately large and the canals poorly raised and inconspicuous. The posterior lacerate foramina are relatively small while the entocarotid foramina are large and exposed. Maxillary vacuities extend from the level of the M^1 paracone root back as far as the level of the M^3 metacone root. The premaxillary vacuities extend as far back as the P^2 anterior root.

Comments. We recommend the following common name to be used in association with *A. mimetes*: Mainland Dusky Antechinus.

Antechinus mimetes insulanus Davison, 1991 new combination

Antechinus swainsonii insulanus Davison, 1991

Description. Davison (1991) provides a detailed description of the holotype.

Rediagnosis of Subspecies. *Antechinus mimetes insulanus* is distinguished from all other taxa in the *A. swainsonii* complex as recognised here, as detailed in the rediagnosis of the nominate form and also in the *A. vandycki* sp. nov. diagnosis.

SPECIES COMPARISONS

In total, more than 300 (male and female) specimens were examined for variation across the full suite of craniodental morphological characters in the 15 antechinus species. These combined data are from AMB's cumulative data set taken from both museum voucher and live specimens. The specimens encompassed the latitudinal geographic range of each species to represent maximal geographic variation and where possible at least 10 males and females of each species were examined for craniodental variation. However, for some species, such as *A. arktos* and *A. vandycki* sp. nov. in the Dusky Antechinus complex, fewer than 10 specimens of each sex were available, despite accessing all registered museum specimens across Australia and conducting numerous field surveys across several years, representing many thousands of trap-nights.

All tests for normality and variance homogeneity of samples used in morphometric analyses were non-significant at $p=0.05$.

Phylogenetic Structure

Figures 2-3 suggest that there are 15 putative species within antechinus. The phylogenies show the four species comprising the Dusky Antechinus complex and *A. minimus* clade is well-supported and deeply divergent compared with all congeners. Each of the four species of Dusky Antechinus and *A. minimus* are strongly supported and monophyletic with respect to each other; however, sister relationships between these taxa are unclear with the exception of the well-supported sister Dusky Antechinus from Tasmania, *A. swainsonii* and *A. vandycki* sp. nov. (Figs 2-3). Within the Dusky Antechinus complex, the four species all form deep and well-supported clades with respect to each other, and within *Au*gence between the two subspecies, *A. m. mimetes* and *A. m. insulanus*; since there was only a single haplotype obtained for *A. mimetes insulanus* (despite the fact that several individuals from two locations were sequenced), it is unclear if these taxa would form well-supported, reciprocally monophyletic clades. Fig. 2 is a phylogeny generated from mitochondrial (Cytochrome B - CytB) data and Fig. 3 combines the data from one mitochondrial gene (Cytochrome B - CytB) and one nuclear gene (Interphotoreceptor Binding Protein - IRBP); both phylogenies concord in their structuring of proposed species clades which then form the basis for testing individual assignment based on craniodental variation in multivariate analyses. Although the majority of the phylogenetic signal is generated from the mtDNA data, the nuclear gene corroborates the interspecific mitochondrial clade structure.

Bivariate Scatterplots

A range of scatterplots are shown for dental variables differentiating *A. swainsonii* from the other three species (four taxa) of Dusky Antechinus. Figs 4-7 show differences among these taxa for a range of the most discriminating dental characters: APV, IPV and NWR, for males and females. The best skull characters for discriminating members of the Dusky Antechinus complex are the front / rear palatal vacuity lengths (APV, PPV) and the size of the gap separating them (IPV) – larger vacuities and

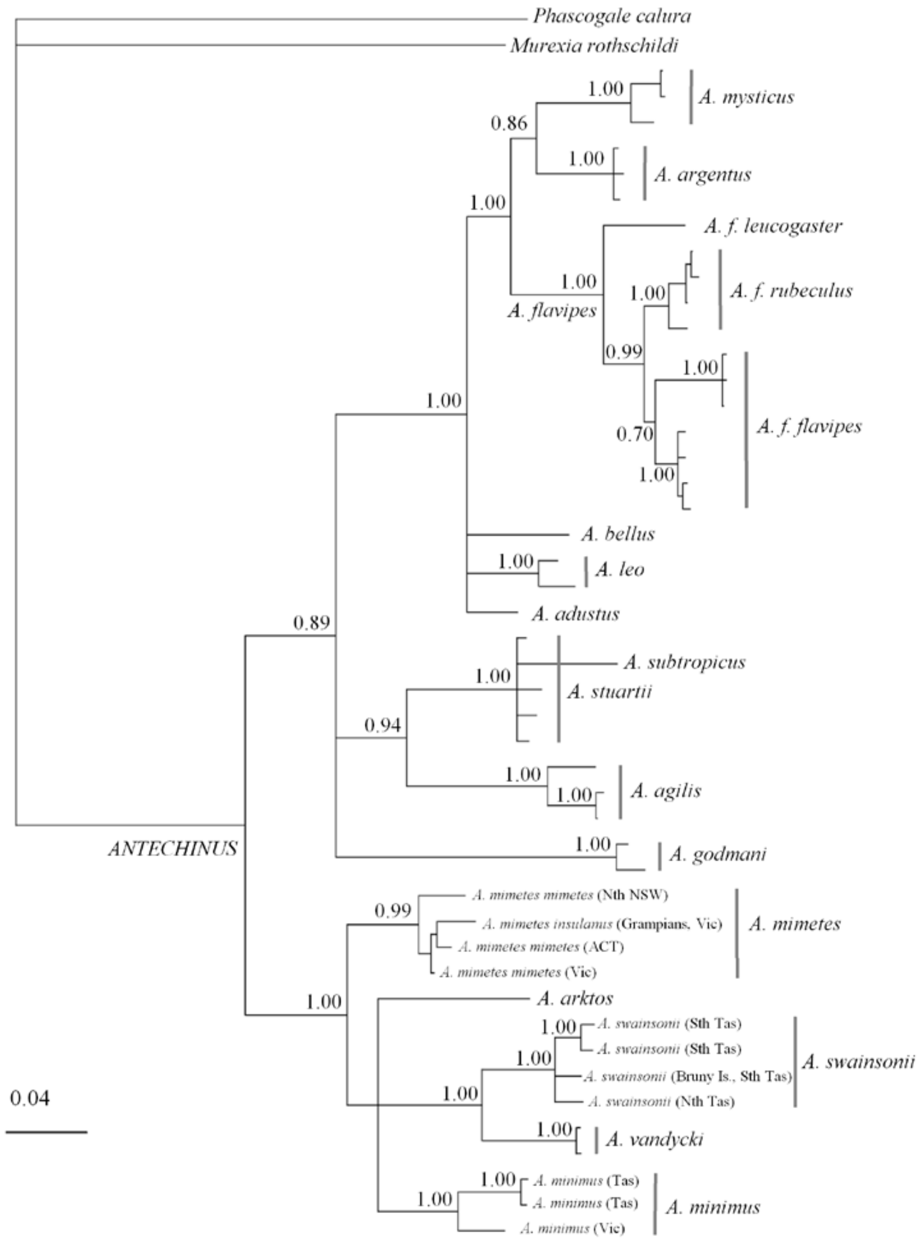

FIG. 2. Bayesian phylogeny of the genus *Antechinus* based on mitochondrial (Cytb) gene sequences. Posterior probabilities are shown at each node (those less than 0.70 are omitted).

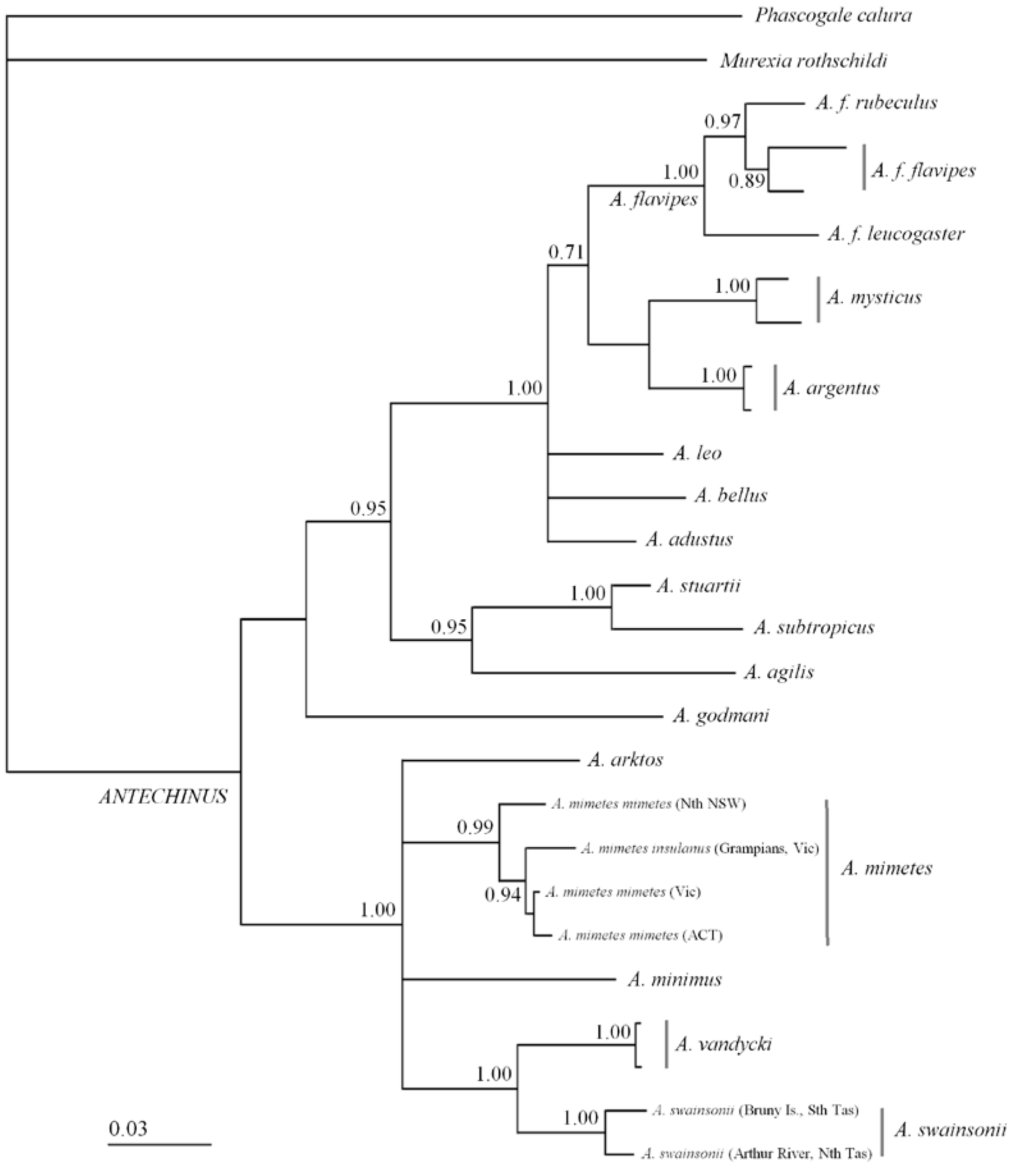

FIG. 3. Bayesian phylogeny of the genus *Antechinus* based on concatenated mitochondrial (Cytb) and nuclear (IRBP) gene sequences. Posterior probabilities are shown at each node (those less than 0.70 are omitted).

smaller separating gaps tend to be a feature of higher latitude species, with smaller holes and larger gaps as one moves into lower latitudes. *Antechinus vandycki* sp. nov. has larger anterior palatal vacuities than any congener.

DFA and CVA

Discriminant Function Analysis (DFA) of members of the Dusky Antechinus complex indicated that 100% of females and males were clustered into the 5 proposed taxon groups

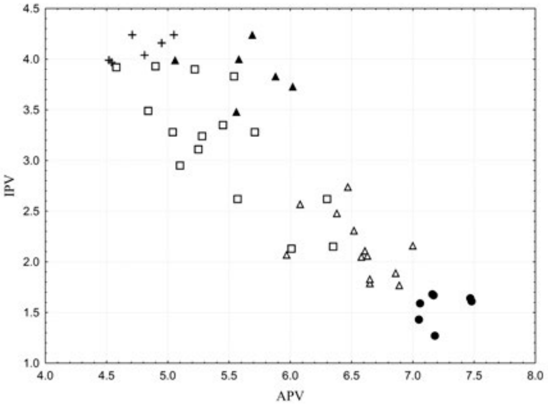

FIG. 4. Scatterplot of anterior palatal vacuity length (APV) versus inter palatal vacuity distance (IPV) measures for male *A. swainsonii* (open triangles), *A. vandycki* sp. nov. (closed circles), *A. mimetes mimetes* (open squares), *A. mimetes insulanus* (closed triangles) and *A. arktos* (crosses).

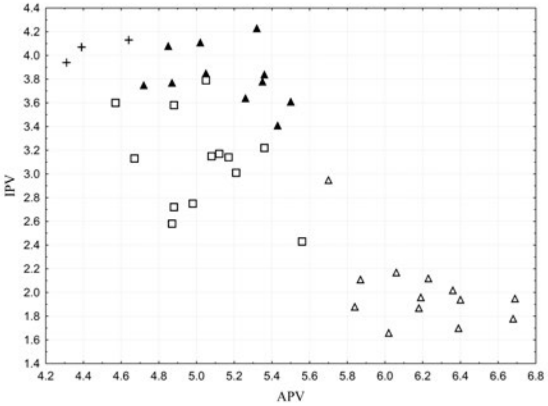

FIG. 5. Scatterplot of anterior palatal vacuity length (APV) versus inter palatal vacuity distance (IPV) measures for female *A. swainsonii* (open triangles), *A. mimetes mimetes* (open squares), *A. mimetes insulanus* (closed triangles) and *A. arktos* (crosses).

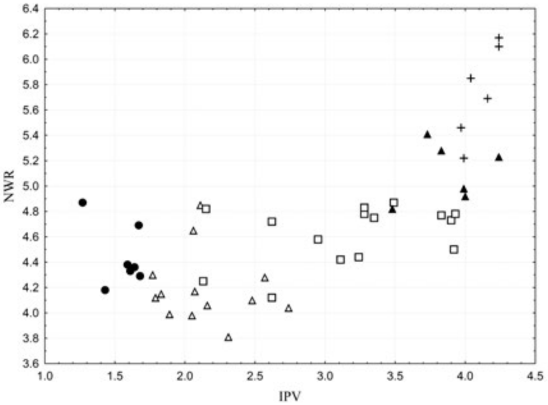

FIG. 6. Scatterplot of inter palatal vacuity distance (IPV) versus width of nasals at the nasal/maxilla /frontal junction (NWR) measures for male *A. swainsonii* (open triangles), *A.vandycki* sp. nov. (closed circles), *A. mimetes mimetes* (open squares), *A. mimetes insulanus* (closed triangles) and *A. arktos* (crosses).

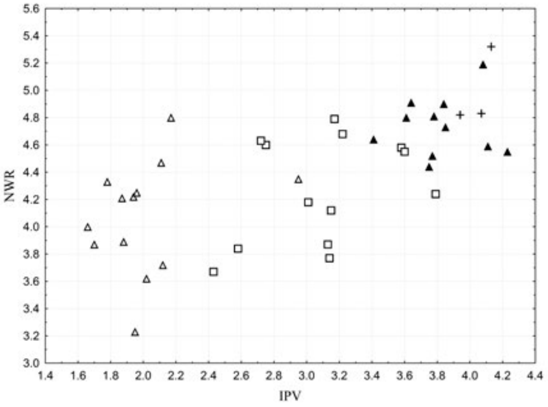

FIG. 7. Scatterplot of inter palatal vacuity distance (IPV) versus width of nasals at the nasal / maxilla /frontal junction (NWR) measures for female *A. swainsonii* (open triangles), *A. mimetes mimetes* (open squares), *A. mimetes insulanus* (closed triangles) and *A. arktos* (crosses).

(*A. swainsonii*, *A. vandycki* sp. nov. *Antechinus mimetes mimetes*, *A. mimetes insulanus* and *A. arktos*) correctly (posterior probabilities all equal to 1.00, not shown), based on the Mahalanobis distance of each individual from the centroid of the *a priori* species group. For CVA, 100% of the variation in dental characters was explained in the first three canonical roots for males and females. Variation was very well resolved for both sexes, as eigenvalues for

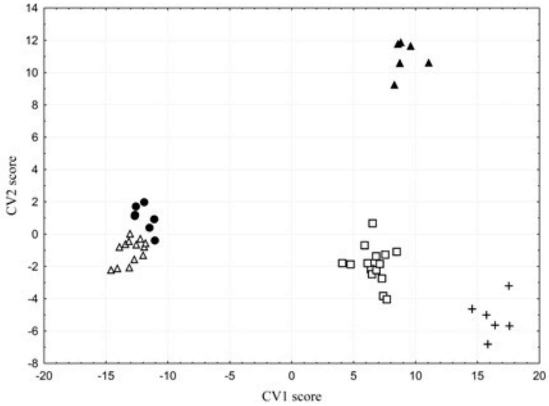

FIG. 8. Scatterplot of canonical variates scores (roots 1 and 2) for male *A. swainsonii* (open triangles), *A. vandycki* sp. nov. (closed circles), *A. mimetes mimetes* (open squares), *A. mimetes insulanus* (closed triangles) and *A. arktos* (crosses).

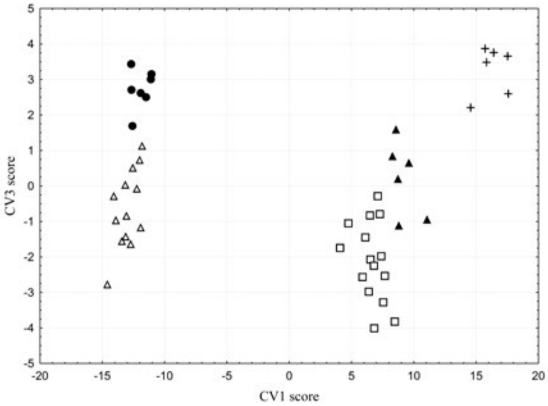

FIG. 9. Scatterplot of canonical variates scores (roots 1 and 3) for male *A. swainsonii* (open triangles), *A. vandycki* sp. nov. (closed circles), *A. mimetes mimetes* (open squares), *A. mimetes insulanus* (closed triangles) and *A. arktos* (crosses).

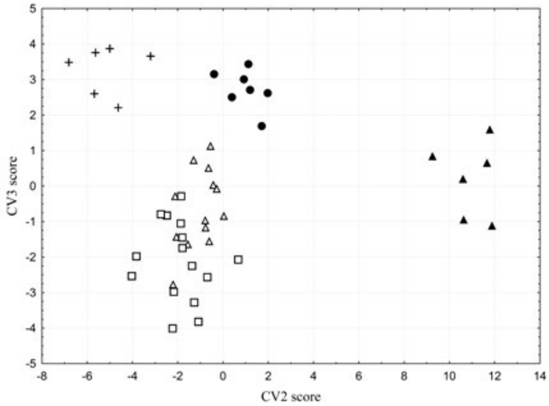

FIG. 10. Scatterplot of canonical variates scores (roots 2 and 3) for male *A. swainsonii* (open triangles), *A. vandycki* sp. nov. (closed circles), *A. mimetes mimetes* (open squares), *A. mimetes insulanus* (closed triangles) and *A. arktos* (crosses).

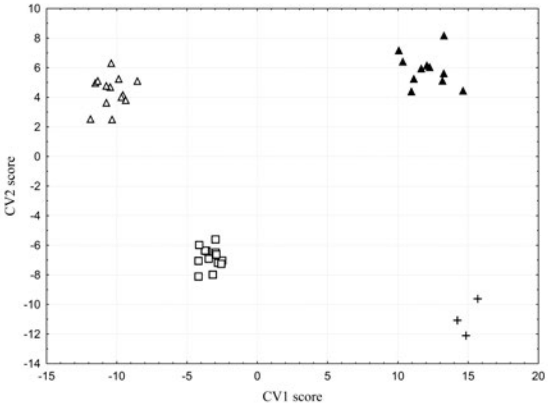

FIG. 11. Scatterplot of canonical variates scores (roots 1 and 2) for female *A. swainsonii* (open triangles), *A. mimetes mimetes* (open squares), *A. mimetes insulanus* (closed triangles) and *A. arktos* (crosses).

the first three canonical roots were well above 1 (males: root 1 = 141.2; root 2 = 22.8; root 3 = 4.5; females: root 1 = 105.7; root 2 = 44.4; root 3 = 4.0) and about four-fifths of the variation was explained in the first root (82%) for males, whereas about two-thirds (69%) was explained in the first root for females. Further, cumulatively the first two roots explained 96% of variation in males and 97% in females. Figs 8-12 show scatterplots of canonical roots 1-3, for males and females; all four taxa are tightly clustered within their taxon and well separated between taxa, for both sexes. Canonical analysis suggests that *A. vandycki* sp. nov. most closely resembles *A. swainsonii* and to a lesser extent *A. mimetes mimetes* and *A. m. insulanus* / *A. arktos*, which reflects their relative geographical proximities. This is a reflection of the longer,

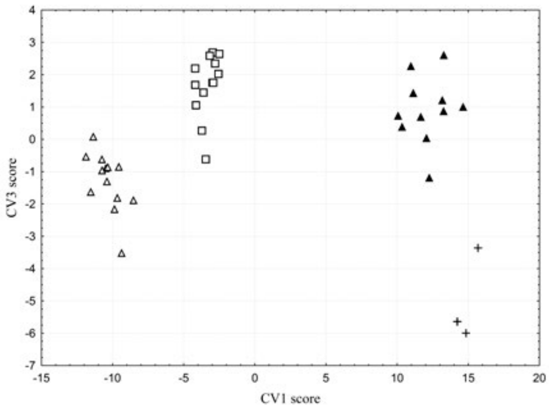

FIG. 12. Scatterplot of canonical variates scores (roots 1 and 3) for female *A. swainsonii* (open triangles), *A. mimetes mimetes* (open squares), *A. mimetes insulanus* (closed triangles) and *A. arktos* (crosses).

more narrow-snouted skulls with larger palatal vacuities characteristic of *A. swainsonii* and *A. vandycki* sp. nov. compared to the stouter skulls of *A. mimetes mimetes* and even more robust *A. mimetes insulanus* and *A. arktos*.

To facilitate direct comparison, univariate statistics (means, standard deviations, range minima and maxima) are shown for each of the external and craniodental measurements for all four species (and 5 taxa) within the Dusky Antechinus species complex: *A. swainsonii*, *A. vandycki* sp. nov., *A. mimetes mimetes*, *A. mimetes insulanus* and *A. arktos.* (refer Tables 1-5). All ANOVAs of measured variables among all antechinus species were significant (Table 6). In pairwise comparisons below, attention is given to diagnosing absolute differences (with no overlap in ranges) where they exist, compared to those that are significantly ($P < 0.05$) different. *Antechinus swainsonii*, with primacy of discovery (Waterhouse 1840) within the complex, was chosen as the reference species, to which all other congeners are compared in pairwise fashion below.

Taxon Comparisons

Antechinus swainsonii (Waterhouse) versus *Antechinus vandycki* sp. nov. Baker, Mutton, Mason and Gray

Pelage. Both species are greyish-brown in appearance; moderate-dark grey on the back, pale grey on the sides and light grey-white on the underside with brownish highlights on the body that are more notable on the flanks and also with brownish warming towards the rump. The tail in both species is bicoloured. However, *A. swainsonii* is distinctly paler than *A. vandycki* sp. nov.; *A. swainsonii* is slightly lighter grey dorsally, lighter grey on the cheeks, shoulders and throat; the underside of *A. swainsonii* is paler grey-white and the feet are lighter, appearing lighter brownish than those in *A. vandycki* sp. nov. The tail is more subtly bicoloured in *A. swainsonii*, with a lighter grey dorsally on the tail. *Antechinus swainsonii* is slightly more lightish grey in the front half of the body merging towards more distinct and slightly warmer brown on the rump, when compared with *A. vandycki* sp. nov.

External Measurements. *Antechinus swainsonii* and *A. vandycki* sp. nov. males are similar in external size (see Tables 1, 2 and 6).

Craniodental Characters. *Antechinus swainsonii* is smaller than *A. vandycki* sp. nov. in absolute measurement (i.e., with no overlap in ranges) for APV in males. *Antechinus swainsonii* is larger than *A. vandycki* sp. nov. in absolute measurement for IPV in males. *Antechinus swainsonii* is significantly smaller than *A. vandycki* sp. nov. for PPV in males (Tables 1, 2 and 6).

Comments. *Antechinus swainsonii* occur throughout most of Tasmania, except the far south-east on Tasman Peninsula. *Antechinus vandycki* sp. nov. have been found to date only in small patches of undisturbed forest on the east of Tasman Peninsula, Tasmania. Genetics: uncorrected pairwise difference at the mitochondrial gene CytB between *A. swainsonii* and *A. vandycki* sp. nov. is 7.3 - 8.6%.

Antechinus swainsonii versus *Antechinus mimetes mimetes* (Thomas) new status

Pelage. *Antechinus swainsonii* is greyish-brown in appearance, greyer at the front with a brownish warming on the rump whereas *A. mimetes mimetes* is more evenly brownish from head to rump. *Antechinus swainsonii* is light greyish on the belly, whereas *A. mimetes mimetes* tends to be light brownish on the belly.

External Measurements. *Antechinus swainsonii* and *A. mimetes mimetes* are similar in external size for males and females (see Tables 1, 3 and 6).

Craniodental Characters. *Antechinus swainsonii* is larger than *A. mimetes mimetes* in absolute measurement for APV in females. *Antechinus swainsonii* is significantly smaller than *A. mimetes mimetes* for IPV in males and females and for TC in males and significantly larger in APV for males (Tables 1, 3 and 6).

Comments. *Antechinus swainsonii* occur throughout most of Tasmania, except the far south-east on Tasman Peninsula. *Antechinus mimetes mimetes* is found on mainland Australia in Victoria and New South Wales. Genetics: uncorrected pairwise difference at the mitochondrial gene CytB between *A. swainsonii* and *A. mimetes mimetes* is 9.4 – 11.4%.

Antechinus swainsonii versus *Antechinus mimetes insulanus* Davison new status

Pelage. *Antechinus swainsonii* is greyish-brown in appearance, greyer at the front with a brownish warming on the rump whereas *A. mimetes insulanus* is more evenly brownish from head to rump. *Antechinus swainsonii* is light greyish on the belly, whereas *A. mimetes insulanus* tends to be light brownish on the belly.

External measurements. *Antechinus swainsonii* and *A. mimetes insulanus* are similar in external size for males and females (see Tables 1, 4 and 6).

Craniodental Characters. *Antechinus swainsonii* is smaller than *A. mimetes insulanus* in absolute measurement for IPV, M^2W, R-LM^3, TC, UML and LML in males and IPV, M^2W, ZW and M_2W in females. *Antechinus swainsonii* is larger than *A. mimetes insulanus* in absolute measurement for APV in females. *Antechinus swainsonii* is significantly smaller than *A. mimetes insulanus* for Dent, IBW, NW, OBW, R-LM^1T, NWR and PML in males and females and in BL, ZW, HT-B and M_2W in males only and R-LM^3, HT, TC, UML and LML in females only. *Antechinus swainsonii* is significantly larger than *A. mimetes insulanus* for APV in males (Tables 1, 3 and 6).

Comments. *Antechinus swainsonii* occur throughout most of Tasmania, except the far south-east on Tasman Peninsula. *Antechinus mimetes insulanus* is found on mainland Australia in the Grampians NP, Victoria. Genetics: uncorrected pairwise difference at the mitochondrial gene CytB between *A. swainsonii* and *A. mimetes insulanus* is 11.0 - 11.6%.

Antechinus swainsonii versus *Antechinus arktos*
Baker, Mutton, Hines and Van Dyck

Pelage. *Antechinus swainsonii* is greyish-brown in appearance, greyer at the front with a brownish warming on the rump whereas *A. arktos* is more brownish from head to rump with a very warm orangish rump and some orange fur around the eye. *Antechinus swainsonii* is light greyish on the belly, whereas *A. arktos* tends to be light brownish on the belly. *Antechinus swainsonii* has brownish hindfeet and a greyish-brown tail, whereas *A. arktos* has black hindfeet and tail.

External Measurements. *Antechinus swainsonii* has significantly smaller tail-vent length than *A. arktos* in males. *Antechinus swainsonii* and *A. arktos* are otherwise similar in external size for males and females (see Tables 1, 5 and 6).

Craniodental Characters. *Antechinus swainsonii* is smaller than *A. arktos* in absolute measurement for IBW, IPV, M^2W, NW, R-LM^1, TC, NWR and UML in males and IPV and UML in females. *Antechinus swainsonii* is larger than *A. arktos* in absolute measurement for APV in males and females. *Antechinus swainsonii* is significantly smaller than *A. arktos* for OBW and R-LM^3 in males only (Tables 1, 5 and 6).

Comments. *Antechinus swainsonii* occur throughout most of Tasmania, except the far south-east on Tasman Peninsula. *Antechinus arktos* is

FIG. 13. *Antechinus swainsonii* holotype specimen photographs of study skin BMNH 60.1.5.18 (male) (A-B): A, top view; B, bottom view. Photographs by Andrew Baker.

found on the border of Qld and NSW in the Tweed Volcano Caldera. Genetics: uncorrected pairwise difference at the mitochondrial gene CytB between *A. swainsonii* and *A. arktos* is 10.8 - 11.8%.

Antechinus swainsonii versus *Antechinus minimus* (Geoffroy)

Pelage. *Antechinus swainsonii* is greyish-brown in appearance, greyer at the front with a brownish warming on the rump whereas *A. minimus* has coarser fur and a leaden grey head that merges to brownish yellow fur on the rump and flanks.

External Measurements. *Antechinus swainsonii* has significantly larger tail-vent length and hindfoot length than *A. minimus* in males and females. (see Tables 1 and 6).

Craniodental Characters. *Antechinus swainsonii* is smaller than *A. minimus* in absolute measurement for IPV in males. *Antechinus swainsonii* is larger than *A. minimus* in absolute measurement for APV, IOW, PL, I^1-P^3, I$_1$-P$_3$ and UPL in males and APV, I^1-P^3, I$_1$-P$_3$ and UPL in females. *Antechinus swainsonii* is significantly smaller than *A. minimus* for R-LC^1 and R-LM^1 in males and IPV, R-LC^1, R-LM^1, R-LM^2 and SWR-LC^{1}B in females. *Antechinus swainsonii* is significantly larger than *A. minimus* for Dent, UML and LML in males and BL, Dent, IOW, PL, UML and LML in females (Tables 1 and 6).

Comments. *Antechinus swainsonii* occur throughout most of Tasmania, except the far south-east on Tasman Peninsula. *Antechinus minimus* is found in both Tasmania, Victoria and SA. In Tasmania, the two species may co-occur although *A. minimus* tends to be found in lower and more open habitats than *A. swainsonii*. Genetics: uncorrected pairwise difference at the mitochondrial gene CytB between *A. swainsonii* and *A. minimus* is 10.0 – 12.0%.

Antechinus swainsonii versus *Antechinus adustus* (Thomas)

Pelage. *Antechinus swainsonii* is greyish-brown in appearance, greyer at the front with a brownish warming on the rump whereas *A. adustus* has more uniformly dark brown fur with rusty tips on the head and back.

External Measurements. *Antechinus swainsonii* is larger than *A. adustus* in absolute measurement for body weight in males and females and in head-body length in females only. *Antechinus swainsonii* has significantly larger head-body length and hindfoot length than *A. adustus* in males only (see Tables 1 and 6).

Craniodental Characters. *Antechinus swainsonii* is smaller than *A. adustus* in absolute measurement for IPV in males and females. *Antechinus swainsonii* is larger than *A. adustus* in absolute measurement for APV, BL, Dent, IOW, HT, PL, HT-B, I^1-P^3, I_1-P_3 and UPL in males and females and PML in females only. *Antechinus swainsonii* is significantly smaller than *A. adustus* for R-LC^1 and SWR-LC^1B in males and females. *Antechinus swainsonii* is significantly larger than *A. adustus* for PML, UML and LML in males and OBW, UML, BuL and LML in females (Tables 1 and 6).

Comments. *Antechinus swainsonii* occur throughout most of Tasmania, except the far south-east on Tasman Peninsula. *Antechinus adustus* is found in the wet tropics of north-east Qld. Genetics: uncorrected pairwise difference at the mitochondrial gene CytB between *A. swainsonii* and *A. adustus* is 14.7 – 16.3%.

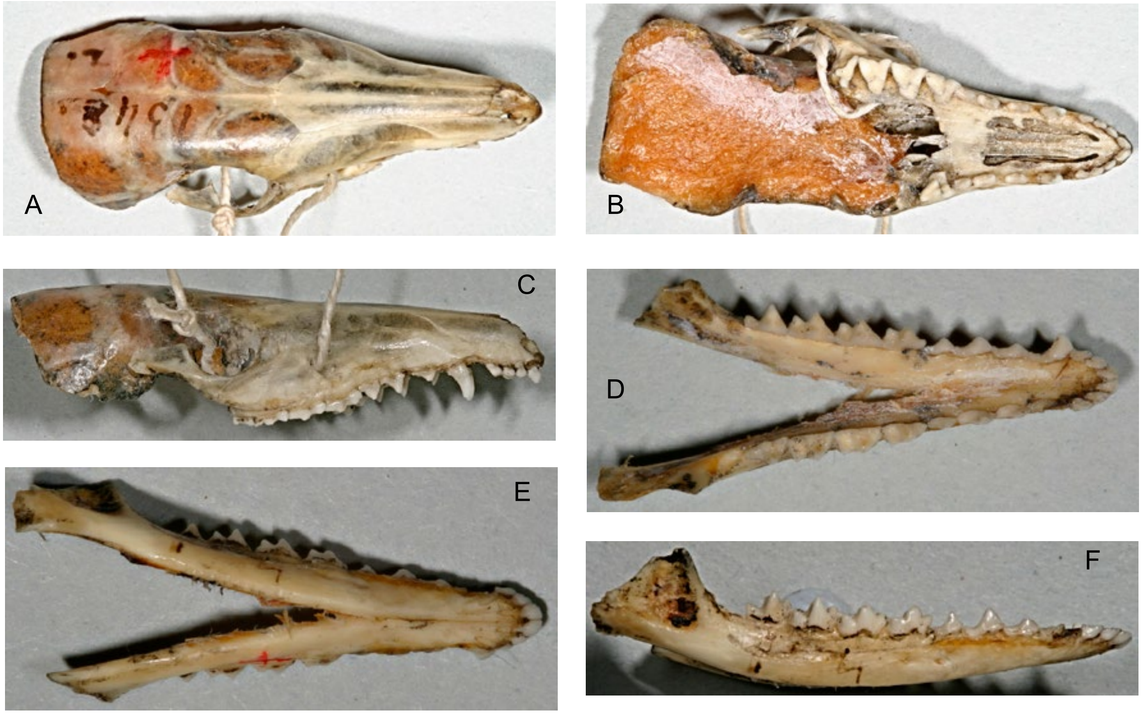

FIG. 14. *Antechinus swainsonii* holotype specimen photographs of skull and dentary BMNH 60.1.5.26 (male) (A-F): A, skull, top view; B, skull, bottom view; C, skull, side view; D, dentary, top view; E, dentary, bottom view; F, dentary, side view. Photographs by Andrew Baker.

FIG. 15. *Antechinus mimetes mimetes* holotype specimen photographs of study skin BMNH 24.10.1.1 (female) (A-B): A, top view; B, bottom view. Photographs by Andrew Baker.

***Antechinus swainsonii* versus *Antechinus agilis* Dickman, Parnaby, Crowther and King**

Pelage. *Antechinus swainsonii* is greyish-brown in appearance, greyer at the front with a brownish warming on the rump whereas *A. agilis* is a uniform medium grey to greyish brown from head to rump. *Antechinus agilis* also has a light-coloured ring of fur around the eyes.

External Measurements. *Antechinus swainsonii* is larger than *A. agilis* in absolute measurement for body weight and hindfoot length in males and in body weight and head-body length in females. *Antechinus swainsonii* has significantly larger head-body length in males and hindfoot length in females (see Tables 1 and 6).

Craniodental Characters. *Antechinus swainsonii* is smaller than *A. agilis* in absolute measurement for IPV in males and females. *Antechinus swainsonii* is larger than *A. agilis* in absolute measurement for APV, BL, Dent, IOW, PL, HT-B, I^1-P^3, LML, I_1-P_3 and UPL in males and APV, BL, Dent, IBW, IOW, HT, PL, HT-B, I^1-P^3, I_1-P_3 and UPL in females. *Antechinus swainsonii* is significantly smaller than *A. agilis* for R-LC^1, R-LM^2 and SWR-LC^{1}B in females. *Antechinus swainsonii* is significantly larger than *A. agilis* for IBW, OBW, PPV, HT, PML, UML and M$_2$W in males and OBW, PPV, NWR, PML, UML and LML in females (Tables 1 and 6).

Comments. *Antechinus swainsonii* occur throughout most of Tasmania, except the far south-east on Tasman Peninsula, whereas *A. agilis* is known only from south-eastern Australia, south of around Sydney's (NSW) latitude. Genetics: uncorrected pairwise difference at the mitochondrial gene CytB between *A. swainsonii* and *A. agilis* is 14.7 – 16.9%.

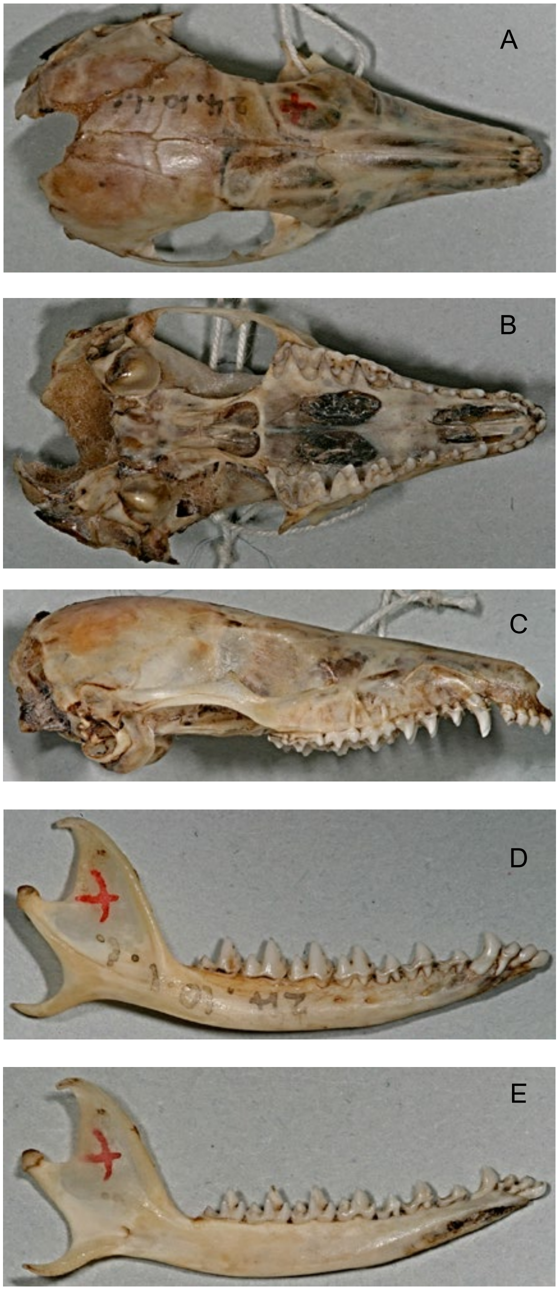

FIG. 16. *Antechinus mimetes mimetes* holotype specimen photographs of skull and dentary BMNH 24.10.1.1 (female) (A-E): A, skull, top view; B, skull, bottom view; C, skull, side view; D, dentary, outside view; E, dentary, inside view. Photographs by Andrew Baker.

Antechinus swainsonii versus *Antechinus argentus* Baker, Mutton and Hines

Pelage. *Antechinus swainsonii* is greyish-brown in appearance, greyer at the front with a brownish warming on the rump whereas *A. argentus* has a silvery head and neck that merge subtly to deep olive-buff coloured fur on the rump and flanks.

External Measurements. *Antechinus swainsonii* is larger than *A. argentus* in absolute measurement for head-body length and hindfoot length in males and in body weight, head-body length and hindfoot length in females (see Tables 1 and 6).

Craniodental Characters. *Antechinus swainsonii* is smaller than *A. argentus* in absolute measurement for IPV, R-LM^1 and R-LM^2 in males and in IPV for females. *Antechinus swainsonii* is larger than *A. argentus* in absolute measurement for APV, BL, Dent, IOW, HT, PL, HT-B, I^1-P^3, I$_1$-P$_3$ and UPL in males and females and in PPV for females only. *Antechinus swainsonii* is significantly smaller than *A. argentus* for R-LC^1, R-LM^3 and SWR-LC^{1}B in males only. *Antechinus swainsonii* is significantly larger than *A. argentus* for LML in males only (Tables 1 and 6).

Comments. *Antechinus swainsonii* occur throughout most of Tasmania, except the far south-east on Tasman Peninsula, whereas *A. argentus* is known only from Kroombit Tops NP in south-east Qld. Genetics: uncorrected pairwise difference at the mitochondrial gene CytB between *A. swainsonii* and *A. argentus* is 16.0 – 17.1%.

Antechinus swainsonii versus *Antechinus bellus* (Thomas)

Pelage. *Antechinus swainsonii* is greyish-brown in appearance, greyer at the front with a brownish warming on the rump whereas *A. bellus* is pale to medium grey above, sometimes with a fawn tinge, with pale grey belly, hands and feet.

FIG. 17. *Antechinus vandycki* sp. nov. holotype specimen photographs of study skin QM JM 20111 (male) (A-B): A, top view; B, bottom view. Photographs by Andrew Baker.

External Measurements. *Antechinus swainsonii* is smaller than *A. bellus* in absolute measurement for ear length in females. *Antechinus swainsonii* is significantly smaller than *A. bellus* in tail-vent length in males and females and in ear length for males. *Antechinus swainsonii* is significantly larger than *A. bellus* in body weight for females (see Tables 1 and 6).

Craniodental Characters. *Antechinus swainsonii* is smaller than *A. bellus* in absolute measurement for IPV, M^{2}W, NW, R-LC^1, R-LM^1, R-LM^2, R-LM^3, SWR-LC^{1}B and BuL for males and females and in M$_2$W in females. *Antechinus swainsonii* is larger than *A. bellus* in absolute measurement for IPV, IOW, I$_1$-P$_3$ and UPL in males and for APV, IBW, IOW, PPV, I^1-P^3, I$_1$-P$_3$ and UPL in females. *Antechinus swainsonii* is significantly smaller than *A. bellus* for OBW, R-LM^{1}T, ZW and M$_2$W in males and for OBW, R-LM^{1}T, ZW, UML and LML in females. *Antechinus swainsonii* is significantly larger than *A. bellus* for IBW, PPV and I^1-P^3 in males and for Dent, PL and HT-B in females (Tables 1 and 6).

Comments. *Antechinus swainsonii* occur throughout most of Tasmania, except the far south-east on Tasman Peninsula, whereas *A. bellus* is known only from northern Northern Territory. Genetics: uncorrected pairwise difference at the mitochondrial gene CytB between *A. swainsonii* and *A. bellus* is 15.9 – 18.3%.

FIG. 18. *Antechinus vandycki* sp. nov. holotype specimen photographs of skull and dentary QM JM 20111 (male) (A-F): A, skull, top view; B, skull, bottom view; C, skull, side view; D, dentary, top view; E, dentary, bottom view; F, dentary, side view. Photographs by Andrew Baker.

Antechnius swainsonii versus *Antechnius flavipes flavipes* (Waterhouse)

Pelage. *Antechinus swainsonii* is greyish-brown in appearance, greyer at the front with a brownish warming on the rump whereas *A. f. flavipes* has marked orange-tonings on the hands, feet and tail base and a pale eye ring.

External Measurements. *Antechinus swainsonii* is significantly larger than *A. flavipes flavipes* in head-body length and hindfoot length for males and females (see Tables 1 and 6).

Craniodental Characters. *Antechinus swainsonii* is smaller than *A. flavipes flavipes* in absolute measurement for IPV, M^{2}W and R-LM^2 in males and for IPV, M^{2}W, R-LC^1, R-LM^2, R-LM^3 and SWR-LC^{1}B in females. *Antechinus swainsonii* is larger than *A. flavipes flavipes* in absolute measurement for APV, IOW, I^1-P^3, I$_1$-P$_3$ and UPL in males and females. *Antechinus swainsonii* is significantly smaller than *A. flavipes flavipes* for NW, R-LC^1, R-LM^1, R-LM^{1}T, R-LM^3, SWR-LC^{1}B, BuL and M$_2$W in males and for NW, R-LM^1, R-LM^{1}T, BuL and M$_2$W in females. *Antechinus swainsonii* is significantly larger than *A. flavipes flavipes* for BL, Dent, IBW, PPV, HT, PL and HT-B for males and females and for PML in females only (see Tables 1 and 6).

Comments. *Antechinus swainsonii* occur throughout most of Tasmania, except the far south-east on Tasman Peninsula, whereas *A. f. flavipes* occurs in a wide range of drier habitat in mainland south-east Australia. Genetics: uncorrected pairwise difference at the mitochondrial gene CytB between *A. swainsonii* and *A. flavipes flavipes* is 15.7 – 17.5%.

Antechnius swainsonii versus *Antechnius flavipes leucogaster* Gray

Pelage. *Antechinus swainsonii* is greyish-brown in appearance, greyer at the front with a brownish warming on the rump whereas *A. f. leucogaster* has marked yellowish-brown fur on the hands, feet and tail base and a pale eyering.

External Measurements. *Antechinus swainsonii* is significantly larger than *A. flavipes leucogaster* in body weight, head-body length and hind-foot length for males and females and for tail-vent length in females (see Tables 1 and 6).

Craniodental Characters. *Antechinus swainsonii* is smaller than *A. flavipes leucogaster* in absolute measurement for IPV, R-LM^1 and R-LM^2 in males and for IPV, R-LC^1, R-LM^1, R-LM^2 and R-LM^3 in females. *Antechinus swainsonii* is larger than *A. flavipes leucogaster* in absolute measurement for APV, IOW, PL, I^1-P^3, I$_1$-P$_3$ and UPL in males and for APV, Dent, IOW, PL, HT-B, I^1-P^3, I$_1$-P$_3$ and UPL in females. *Antechinus swainsonii* is significantly smaller than *A. flavipes leucogaster* for NW, R-LC^1, R-LM^{1}T, R-LM^3, SWR-LC^{1}B and BuL in males and for M^{2}W, NW, R-LM^{1}T, SWR-LC^{1}B, BuL and M$_2$W in females. *Antechinus swainsonii* is significantly larger than *A. flavipes leucogaster* for BL, Dent, IBW, PPV, HT, UML, HT-B and LML in males and for BL, IBW, PPV, HT, PML, UML and LML in females (see Tables 1 and 6).

Comments. *Antechinus swainsonii* occur throughout most of Tasmania, except the far south-east on Tasman Peninsula, whereas *A. flavipes leucogaster* occurs in south-west Western Australia. Genetics: uncorrected pairwise difference at the mitochondrial gene CytB between *A. swainsonii* and *A. flavipes leucogaster* is 15.3 – 17.1%.

Antechnius swainsonii versus *Antechnius flavipes rubeculus* Van Dyck

Pelage. *Antechinus swainsonii* is greyish-brown in appearance, greyer at the front with a brownish warming on the rump whereas *A. flavipes rubeculus* has orange-toned fur on the upper hind feet and tail base and a pale eyering.

External Measurements. *Antechinus swainsonii* is similar in size to *A. flavipes rubeculus* (see Tables 1 and 6).

Craniodental Characters. *Antechinus swainsonii* is smaller than *A. flavipes rubeculus* in absolute measurement for IPV, M^{2}W, R-LC^1, R-LM^1, R-LM^{1}T, R-LM^2 and SWR-LC^{1}B in males and for IPV, M^{2}W, R-LC^1, R-LM^1, R-LM^{1}T, R-LM^2, R-LM^3, ZW, SWR-LC^{1}B, BuL and M$_2$W in females. *Antechinus swainsonii* is larger than *A. flavipes rubeculus* in absolute measurement for APV, IOW, I^1-P^3, I$_1$-P$_3$ and UPL in males and females and for PPV in females. *Antechinus swainsonii* is significantly smaller than *A. flavipes rubeculus* for NW, OBW, R-LM^3, ZW, NWR, UML, BuL and M$_2$W in males and for NW, OBW, UML and LML in females. *Antechinus swainsonii* is significantly larger than *A. flavipes rubeculus* for PL and HT-B in females only (see Tables 1 and 6).

Comments. *Antechinus swainsonii* occur throughout most of Tasmania, except the far south-east on Tasman Peninsula, whereas *A. flavipes rubeculus* is only found in the wet tropics of north-east Qld. Genetics: uncorrected pairwise difference at the mitochondrial gene CytB between *A. swainsonii* and *A. flavipes rubeculus* is 16.1 – 17.9%.

Antechnius swainsonii versus *Antechnius godmani* (Thomas)

Pelage. *Antechinus swainsonii* is greyish-brown in appearance, greyer at the front with a brownish warming on the rump whereas *A. godmani* is more uniformly brown on the head and back with a naked-looking tail.

External Measurements. *Antechinus swainsonii* is significantly smaller than *A. godmani* in body weight and tail-vent length in males and females and in ear length for females (see Tables 1 and 6).

Craniodental Characters. *Antechinus swainsonii* is smaller than *A. godmani* in absolute measurement for IBW, IPV, M^2W, R-LC^1, R-LM^1, R-LM^1T, SWR-LC^1B, TC, UML, LML and M_2W in males and for IPV, M^2W, OBW, R-LC^1, R-LM^1, R-LM^1T, R-LM^2, R-LM^3, ZW, SWR-LC^1B, TC, UML, LML and M_2W in females. *Antechinus swainsonii* is larger than *A. godmani* in absolute measurement for APV in males and females. *Antechinus swainsonii* is significantly smaller than *A. godmani* for BL, Dent, OBW, R-LM^2, R-LM^3, ZW and PL in males and for BL and IBW in females. *Antechinus swainsonii* is significantly larger than *A. godmani* for I_1-P_3 in males and females (see Tables 1 and 6).

Comments. *Antechinus swainsonii* occur throughout most of Tasmania, except the far south-east on Tasman Peninsula, whereas *A. godmani* is known from only the wet tropics in north-east Qld. Genetics: uncorrected pairwise difference at the mitochondrial gene CytB between *A. swainsonii* and *A. godmani* is 16.3 – 19.1%.

Antechnius swainsonii versus
Antechnius leo Van Dyck

Pelage. *Antechinus swainsonii* is greyish-brown in appearance, greyer at the front with a brownish warming on the rump whereas *A. leo* is uniformly cinnamon on the head and back with slightly darkened hair forming a mid-dorsal head stripe.

External Measurements. *Antechinus swainsonii* is significantly smaller than *A. leo* in tail-vent length, hindfoot length and ear length in males and females (see Tables 1 and 6).

Craniodental Characters. *Antechinus swainsonii* is smaller than *A. leo* in absolute measurement for IPV, M^2W, NW, R-LC^1, R-LM^1, R-LM^1T, R-LM^2, R-LM^3, SWR-LC^1B and M_2W in males and for IPV, M^2W, NW, OBW, R-LC^1, R-LM^1, R-LM^1T, R-LM^2, R-LM^3, ZW, SWR-LC^1B, TC and M_2W in females. *Antechinus swainsonii* is larger than *A. leo* in absolute measurement for APV, IOW, I_1-P_3 and UPL in males and females. *Antechinus swainsonii* is significantly smaller than *A. leo* for IBW, OBW, ZW, TC, NWR, PML, UML, BuL and LML in males and for IBW, NWR, UML, BuL and LML in females. *Antechinus swainsonii* is significantly larger than *A. leo* for I_1-P_3 in males and females and HT-B in females (see Tables 1 and 6).

Comments. *Antechinus swainsonii* occur throughout most of Tasmania, except the far south-east on Tasman Peninsula, whereas *A. leo* is known only from north of Princess Charlotte Bay, on Cape York Peninsula in far northern Qld. Genetics: uncorrected pairwise difference at the mitochondrial gene CytB between *A. swainsonii* and *A. leo* is 15.7 – 17.9%.

Antechnius swainsonii versus
Antechnius mysticus Baker, Mutton and Van Dyck

Pelage. *Antechinus swainsonii* is greyish-brown in appearance, greyer at the front with a brownish warming on the rump whereas *A. mysticus* has a greyish-brown head and neck, merging gradually to yellowish-buff on the rump and flanks, with a buff-brown tail base and slightly darkened tip.

External Measurements. *Antechinus swainsonii* is larger than *A. mysticus* in absolute measurement for hindfoot length in males. *Antechinus swainsonii* is significantly larger than *A. mysticus* in head-body length for males and for body weight, head-body length and hindfoot length in females (see Tables 1 and 6).

Craniodental Characters. *Antechinus swainsonii* is smaller than *A. mysticus* in absolute measurement for IPV and R-LC^1 in males and females and for SWR-LC^1B in males. *Antechinus swainsonii* is larger than *A. mysticus* in absolute measurement for APV, IOW, PL, HT-B, I^1-P^3, I_1-P_3 and UPL in males and females and for Dent and HT in females only. *Antechinus swainsonii* is significantly smaller than *A. mysticus* for M^2W, R-LM^1, R-LM^2 and R-LM^3 in males and for M^2W, R-LM^2, R-LM^3 and SWR-LC^1B in females. *Antechinus swainsonii* is significantly larger than *A. mysticus* for BL, Dent, IBW, HT, UML and LML in males and for BL, IBW, PML, UML and LML in females (see Tables 1 and 6).

Comments. *Antechinus swainsonii* occur throughout most of Tasmania, except the far south-east on Tasman Peninsula, whereas *A. mysticus* occurs in scattered coastal populations between the Qld / NSW border in far south-east Qld and Eungella NP near Mackay in mid-east Qld. Genetics: uncorrected pairwise difference at the mitochondrial gene CytB between *A. swainsonii* and *A. mysticus* is 15.5 – 17.5%.

Antechinus swainsonii versus *Antechinus stuartii* Macleay

Pelage. *Antechinus swainsonii* is greyish-brown in appearance, greyer at the front with a brownish warming on the rump whereas *A. stuartii* is more uniformly brownish-grey from head to rump.

External Measurements. *Antechinus swainsonii* is larger than *A. stuartii* in absolute measurement for hindfoot length in males and for body weight and head-body length in females. *Antechinus swainsonii* is significantly larger than *A. stuartii* in body weight and head-body length in males and for hind-foot length in females (see Tables 1 and 6).

Craniodental Characters. *Antechinus swainsonii* is smaller than *A. stuartii* in absolute measurement for IPV in males only. *Antechinus swainsonii* is larger than *A. stuartii* in absolute measurement for APV, IOW, PL, I^1-P^3, I_1-P_3 and UPL in males and for APV, BL, Dent, IBW, IOW, HT, PL, HT-B, I^1-P^3, I_1-P_3 and UPL in females. *Antechinus swainsonii* is significantly smaller than *A. stuartii* for R-LC^1 and SWR-LC^1B in males and females and for IPV in females. *Antechinus swainsonii* is significantly larger than *A. stuartii* for BL, Dent, IBW, HT, PML, UML, HT-B and LML in males and for OBW, NWR, PML, UML and LML in females (see Tables 1 and 6).

Comments. *Antechinus swainsonii* occur throughout most of Tasmania, except the far south-east on Tasman Peninsula, *A. stuartii* occurs only on mainland Australia, in eastern NSW north of about Sydney to far south-east Queensland (Girraween NP, Lamington NP, Main Range NP, Springbrook NP and Tamborine NP). Genetics: uncorrected pairwise difference at the mitochondrial gene CytB between *A. swainsonii* and *A. stuartii* is 13.4 – 15.9%.

Antechinus swainsonii versus *Antechinus subtropicus* Van Dyck and Crowther

Pelage. *Antechinus swainsonii* is greyish-brown in appearance, greyer at the front with a brownish warming on the rump whereas *A. subtropicus* is more uniformly brownish from head to rump.

External Measurements. *Antechinus swainsonii* is significantly larger than *A. subtropicus* in hindfoot length in males and for head-body length in females (see Tables 1 and 6).

Craniodental Characters. *Antechinus swainsonii* is larger than *A. subtropicus* in absolute measurement for APV, IOW, I^1-P^3, I_1-P_3 and UPL in males and females and for HT-B in females only. *Antechinus swainsonii* is significantly smaller than *A. subtropicus* for M^2W, PPV, R-LC^1, SWR-LC^1B and TC in males and for M^2W, PPV, R-LC^1, SWR-LC^1B and M_2W for females. *Antechinus swainsonii* is significantly larger than *A. subtropicus* for BL, Dent, HT and PL for males and females and for HT-B and LML for males only (see Tables 1 and 6).

Comments. *Antechinus swainsonii* occur throughout most of Tasmania, except the far south-east on Tasman Peninsula, whereas *A. subtropicus* appears to have a more subtropical distribution, occurring from Gympie south-east Qld south to Border Ranges NP in north-east NSW. Genetics: uncorrected pairwise difference at the mitochondrial gene CytB between *A. swainsonii* and *A. subtropicus* is 14.5 – 16.8%.

DISCUSSION

Systematics

The phylogenies reconstructed here (Figs 2-3) provide evidence of 15 putative species

TABLE 1. Univariate statistics: means, standard deviations and range minima and maxima of measured variables for *Antechinus swainsonii*.

MALES						FEMALES					
	Valid N	Mean	Min	Max	St. Dev.		Valid N	Mean	Min	Max	St. Dev.
wt	11	63.16	42.30	93.00	14.53	wt	15	41.59	31.00	57.00	7.36
hb	12	133.61	111.30	161.00	13.06	hb	16	116.70	103.19	127.00	8.69
tv	12	97.90	89.00	110.00	6.53	tv	16	87.75	77.00	101.42	6.13
hf	12	21.84	20.00	24.00	1.27	hf	15	19.30	18.00	21.00	0.81
e	12	16.86	15.01	21.00	1.47	e	14	15.28	14.50	16.00	0.54
APV	13	6.56	5.97	7.00	0.29	APV	13	6.20	5.70	6.69	0.30
BL	13	30.29	28.54	32.39	1.27	BL	13	28.70	26.80	30.36	1.17
Dent	13	24.62	23.05	26.61	1.19	Dent	13	23.28	21.74	24.72	0.94
IBW	13	4.50	4.15	4.81	0.19	IBW	13	4.33	4.14	4.65	0.15
IOW	13	7.95	7.61	8.77	0.30	IOW	13	7.84	7.38	8.43	0.34
IPV	13	2.14	1.77	2.74	0.31	IPV	13	2.01	1.66	2.95	0.32
M^{2}W	13	2.29	2.19	2.38	0.06	M^{2}W	13	2.22	2.08	2.34	0.08
NW	13	2.45	2.03	2.85	0.20	NW	13	2.45	2.20	2.73	0.16
OBW	13	12.24	11.31	13.30	0.54	OBW	13	11.80	11.21	12.18	0.29
PPV	13	5.33	4.39	5.99	0.44	PPV	13	5.00	4.52	5.56	0.30
R-LC^1	13	4.64	3.99	5.20	0.33	R-LC^1	13	4.27	3.93	4.56	0.20
R-LM^1	13	8.52	7.70	9.07	0.47	R-LM^1	13	8.32	7.78	8.67	0.31
R-LM^{1}T	13	7.64	7.08	8.10	0.36	R-LM^{1}T	13	7.35	6.99	7.72	0.25
R-LM^2	13	10.42	9.58	11.27	0.51	R-LM^2	13	10.01	9.48	10.51	0.30
R-LM^3	13	12.73	11.89	13.64	0.53	R-LM^3	13	12.17	11.21	12.59	0.40
ZW	13	16.68	15.43	18.49	0.97	ZW	13	15.63	14.16	16.42	0.58
HT	13	10.50	9.79	10.99	0.40	HT	13	10.10	9.61	10.77	0.37
PL	13	17.85	16.97	19.19	0.68	PL	13	17.08	15.91	17.87	0.62
SWR-LC^{1}B	13	4.18	3.74	4.75	0.29	SWR-LC^{1}B	13	3.81	3.54	4.16	0.21
TC	13	2.52	2.21	2.91	0.19	TC	13	2.62	2.22	2.87	0.21
NWR	13	4.19	3.81	4.85	0.28	NWR	13	4.07	3.23	4.80	0.41
PML	13	9.11	7.67	10.27	0.74	PML	13	8.62	7.99	10.23	0.75
UML	13	6.87	6.33	7.18	0.23	UML	13	6.65	6.23	7.01	0.29
HT-B	13	8.29	7.71	8.81	0.32	HT-B	13	8.08	7.68	8.52	0.26
BuL	13	4.19	3.62	4.50	0.26	BuL	13	4.02	3.76	4.28	0.16
I^1-P^3	13	10.00	9.43	10.45	0.28	I^1-P^3	13	9.54	8.88	10.12	0.37
LML	13	7.56	7.10	7.88	0.24	LML	13	7.33	6.96	7.71	0.29
I$_1$-P$_3$	13	7.96	7.51	8.43	0.27	I$_1$-P$_3$	13	7.57	7.09	8.03	0.36
M$_2$W	13	2.19	2.00	2.33	0.10	M$_2$W	13	2.09	1.94	2.22	0.08
UPL	13	4.44	4.16	5.08	0.25	UPL	13	4.20	3.86	4.45	0.19

TABLE 2. Univariate statistics: means, standard deviations and range minima and maxima of measured variables for *Antechinus vandycki* sp. nov.

MALES					
	Valid N	Mean	Min	Max	St. Dev.
wt	6	73.08	46.30	92.80	16.87
hb	6	120.21	104.91	132.60	9.82
tv	6	109.06	92.34	118.02	9.39
hf	6	22.47	20.34	24.62	1.67
e	6	16.37	14.94	17.55	1.00
APV	7	7.22	7.05	7.48	0.18
BL	7	31.71	29.90	33.20	1.04
Dent	7	25.92	24.48	27.76	1.02
IBW	7	4.48	4.21	4.75	0.21
IOW	7	7.95	7.67	8.11	0.15
IPV	7	1.56	1.27	1.68	0.15
M^2W	7	2.33	2.24	2.38	0.05
NW	7	2.32	2.21	2.51	0.10
OBW	7	12.64	12.04	13.07	0.35
PPV	7	6.11	5.78	6.54	0.29
R-LC^1	7	4.86	4.66	5.02	0.12
R-LM^1	7	8.68	8.23	9.08	0.34
R-LM^1T	7	7.87	7.61	8.15	0.16
R-LM^2	7	10.55	9.70	10.97	0.47
R-LM^3	7	12.91	12.39	13.44	0.37
ZW	7	17.25	15.99	18.39	0.71
HT	7	10.72	10.36	11.32	0.30
PL	7	18.73	17.89	19.38	0.56
SWR-LC^1B	7	4.36	4.24	4.59	0.14
TC	7	2.66	2.44	2.88	0.18
NWR	7	4.44	4.18	4.87	0.24
PML	7	9.52	8.94	10.21	0.39
UML	7	6.94	6.78	7.08	0.11
HT-B	7	8.46	7.82	8.84	0.34
BuL	7	4.41	4.15	4.57	0.16
I^1-P^3	7	10.49	10.14	11.00	0.30
LML	7	7.58	7.37	7.68	0.11
I_1-P_3	7	8.41	8.18	8.63	0.17
M_2W	7	2.21	2.17	2.27	0.04
UPL	7	4.66	4.45	4.79	0.11

in the genus *Antechinus*. Species delimitations based on *Antechinus* DNA work are necessarily arbitrary, depending on the strength of monophyletic clade support and relative depth/ divergence of clades; all proposed antechinus species clades were distinctly clustered, deeply divergent (5-15% pairwise divergence at mtDNA), bearing strongly supported nodes (0.99-1.00 posterior probabilities).

Our DNA data corroborate the findings of Armstrong *et al.* (1998), who found similarly deep levels of divergence (using combined mtDNA and nDNA) among various antechinus species, including: *A. swainsonii, A. minimus, A. leo, A. bellus, A. godmani, A. flavipes, A.agilis* and *A. stuartii*. The present study provides a comparative analysis that encompasses a range of recently resolved antechinus taxa that could not be included in the work of Armstrong *et al.*: *A. adustus, A. subtropicus, A. mysticus, A. argentus, A. arktos, A. swainsonii* (Tas), *A. vandycki* sp. nov. (Tas), *A. mimetes insulanus* (Grampians, Vic).

Our DNA evidence of species distinction is consistently corroborated by a suite of other data sources, including: morphology (pelage colour, body size and craniodentary), biogeography (allopatric separation and/or relatively deep divergence across limited geographic distance) and/or ecology/behaviour (differences in breeding timing for a genus where breeding is known to be highly synchronised annually within any given species).

Assessing all data, we conclude the total evidence strongly supports the existence of 15 species of antechinus, including four species of Dusky Antechinus.

Our (direct sequencing) genetic work presented here corroborates the preliminary work of Smith (1983), who examined electrophoretic variation in *A. swainsonii* on either side of Bass Strait. He concluded that given a mean genetic distance of 0.085 +- 0.015 the trans-Bassian populations of *A. swainsonii* warranted at minimum subspecific status ('...or further elevation' p. 759). Smith (1983) analysed a total of 18 *A. swainsonii* individuals across a total of 4 populations on mainland Australia (1 in Canberra, 3 in Victoria) and compared them

TABLE 3. Univariate statistics: means, standard deviations and range minima and maxima of measured variables for *Antechinus mimetes mimetes*.

MALES						FEMALES					
	Valid N	Mean	Min	Max	St. Dev.		Valid N	Mean	Min	Max	St. Dev.
wt	6	60.55	42.00	112.00	26.01	wt	8	38.24	30.50	47.80	5.10
hb	20	122.18	89.20	150.00	16.50	hb	27	106.14	85.00	125.00	11.59
tv	20	101.11	82.43	113.75	8.83	tv	27	89.53	76.00	98.00	5.77
hf	20	21.41	18.69	24.00	1.41	hf	26	19.61	17.00	22.00	1.15
e	19	16.56	14.29	20.00	1.63	e	26	15.82	14.08	19.40	1.18
APV	15	5.41	4.58	6.35	0.52	APV	12	5.02	4.57	5.56	0.28
BL	15	30.39	28.53	31.72	0.93	BL	11	28.63	27.33	30.49	0.98
Dent	15	24.67	23.21	25.88	0.79	Dent	12	23.18	22.05	24.30	0.74
IBW	15	4.73	4.35	5.12	0.24	IBW	12	4.46	4.05	4.87	0.25
IOW	15	8.12	7.68	8.51	0.23	IOW	12	7.85	7.21	8.34	0.33
IPV	15	3.19	2.13	3.93	0.60	IPV	12	3.09	2.43	3.79	0.42
M^{2}W	15	2.36	2.20	2.53	0.09	M^{2}W	12	2.25	2.10	2.37	0.07
NW	15	2.70	2.41	2.92	0.15	NW	12	2.54	2.14	3.02	0.24
OBW	15	12.34	11.60	13.33	0.50	OBW	12	11.85	11.11	12.53	0.40
PPV	15	5.41	4.37	6.03	0.48	PPV	12	5.29	4.67	5.71	0.26
R-LC^1	15	4.63	4.34	4.92	0.19	R-LC^1	12	4.34	3.79	4.71	0.26
R-LM^1	15	8.78	8.03	9.39	0.38	R-LM^1	12	8.45	7.68	8.93	0.38
R-LM^{1}T	15	7.68	7.27	8.15	0.29	R-LM^{1}T	12	7.34	6.80	7.63	0.28
R-LM^2	15	10.65	9.63	11.81	0.62	R-LM^2	12	10.24	9.09	11.06	0.68
R-LM^3	15	13.28	12.23	14.39	0.56	R-LM^3	12	12.78	11.15	13.64	0.71
ZW	15	17.00	15.52	18.07	0.77	ZW	12	15.74	14.47	16.94	0.76
HT	15	10.76	10.28	11.15	0.28	HT	12	10.34	9.81	10.92	0.32
PL	15	17.51	16.66	18.27	0.51	PL	12	16.77	15.83	17.69	0.53
SWR-LC^{1}B	15	4.18	3.78	4.63	0.22	SWR-LC^{1}B	12	3.88	3.47	4.29	0.28
TC	15	2.90	2.50	3.41	0.29	TC	12	2.83	2.54	3.36	0.26
NWR	15	4.62	4.12	4.87	0.23	NWR	12	4.23	3.67	4.68	0.37
PML	15	9.39	8.21	10.70	0.69	PML	12	8.60	7.84	9.47	0.54
UML	15	6.93	6.29	7.52	0.34	UML	12	6.72	6.25	7.17	0.26
HT-B	15	8.57	8.21	9.04	0.24	HT-B	12	8.16	7.57	8.55	0.31
BuL	15	4.26	3.93	4.60	0.21	BuL	12	4.06	3.82	4.33	0.18
I^1-P^3	15	9.67	8.98	10.20	0.33	I^1-P^3	12	9.16	8.82	9.90	0.29
LML	15	7.60	7.00	8.19	0.37	LML	12	7.37	6.87	7.73	0.26
I$_1$-P$_3$	15	7.78	7.31	8.08	0.26	I$_1$-P$_3$	12	7.30	6.93	7.75	0.23
M$_2$W	15	2.18	1.98	2.41	0.12	M$_2$W	12	2.13	2.00	2.25	0.08
UPL	15	4.38	4.03	4.70	0.23	UPL	12	4.09	3.61	4.52	0.26

TABLE 4. Univariate statistics: means, standard deviations and range minima and maxima of measured variables for *Antechinus mimetes insulanus*.

MALES						FEMALES					
	Valid N	Mean	Min	Max	St. Dev.		Valid N	Mean	Min	Max	St. Dev.
wt	4	70.63	46.00	87.00	17.55	wt	4	49.75	40.00	60.00	8.26
hb	6	138.87	117.10	165.00	17.48	hb	6	123.20	111.40	144.80	11.35
tv	6	111.86	105.00	121.90	7.62	tv	5	99.49	96.39	106.27	3.88
hf	6	22.04	20.00	24.26	1.49	hf	6	20.50	19.60	21.27	0.60
e	5	17.47	15.45	20.50	1.92	e	6	17.02	14.00	19.40	2.00
APV	6	5.63	5.06	6.02	0.33	APV	11	5.16	4.72	5.50	0.27
BL	6	32.57	30.19	33.85	1.37	BL	11	29.93	28.39	30.74	0.71
Dent	6	26.53	24.68	27.61	1.07	Dent	11	24.37	22.96	25.03	0.56
IBW	6	5.14	4.99	5.34	0.14	IBW	11	4.77	4.55	4.99	0.15
IOW	6	7.94	7.78	8.27	0.17	IOW	11	7.86	7.59	8.08	0.14
IPV	6	3.88	3.48	4.24	0.26	IPV	11	3.82	3.41	4.23	0.24
M^{2}W	6	2.58	2.53	2.65	0.05	M^{2}W	11	2.50	2.44	2.54	0.03
NW	6	2.93	2.77	3.19	0.16	NW	11	2.90	2.61	3.12	0.14
OBW	6	13.41	12.98	13.85	0.35	OBW	11	12.56	11.99	13.33	0.37
PPV	6	5.31	4.60	5.57	0.36	PPV	11	4.92	4.34	5.43	0.36
R-LC^1	6	4.99	4.71	5.26	0.22	R-LC^1	11	4.61	4.32	4.92	0.19
R-LM^1	6	9.07	8.86	9.31	0.16	R-LM^1	11	8.53	8.08	8.78	0.23
R-LM^{1}T	6	8.29	8.01	8.76	0.27	R-LM^{1}T	11	7.92	7.60	8.24	0.19
R-LM^2	6	10.61	10.12	11.43	0.53	R-LM^2	11	9.91	9.28	10.50	0.39
R-LM^3	6	14.09	13.85	14.45	0.23	R-LM^3	11	13.12	12.43	13.86	0.47
ZW	6	18.80	17.83	20.01	0.83	ZW	11	17.09	16.48	17.90	0.47
HT	6	11.20	10.65	11.89	0.46	HT	11	10.66	10.27	10.89	0.21
PL	6	18.84	17.88	19.36	0.53	PL	11	17.78	16.84	18.16	0.43
SWR-LC^{1}B	6	4.47	4.22	4.74	0.21	SWR-LC^{1}B	11	4.10	3.85	4.34	0.16
TC	6	3.11	2.96	3.28	0.14	TC	11	3.07	2.71	3.39	0.22
NWR	6	5.11	4.82	5.41	0.23	NWR	11	4.73	4.44	5.19	0.22
PML	6	10.64	9.90	11.30	0.47	PML	11	9.63	8.84	10.20	0.43
UML	6	7.46	7.35	7.62	0.11	UML	11	7.20	6.96	7.37	0.14
HT-B	6	8.97	8.49	9.48	0.36	HT-B	11	8.30	8.00	8.58	0.18
BuL	6	4.43	4.19	4.73	0.19	BuL	11	4.24	3.99	4.68	0.22
I^1-P^3	6	10.20	9.42	10.61	0.43	I^1-P^3	11	9.54	9.19	9.90	0.25
LML	6	8.13	8.00	8.43	0.17	LML	11	7.91	7.67	8.08	0.13
I$_1$-P$_3$	6	8.33	7.89	8.65	0.31	I$_1$-P$_3$	11	7.59	7.18	7.82	0.21
M$_2$W	6	2.36	2.33	2.43	0.04	M$_2$W	11	2.30	2.24	2.34	0.03
UPL	6	4.55	4.13	4.91	0.29	UPL	11	4.18	3.91	4.57	0.20

to a total of 4 *A. swainsonii* individuals from a total of two populations on Tasmania (Arthur River in the north and Mount Wellington in the south). Although based on small sample sizes, Smith found a striking pattern of markedly greater differentiation between *A. swainsonii* across Bass Strait compared to that among either mainland or Tasmanian populations of *A. swainsonii*.

Our genetic data from the present study indicate that four deeply divergent (pairwise mtDNA 7.5-12.5%) and distinctive species comprise the Dusky Antechinus complex; each species is deeply structured, monophyletic, very strongly supported and taken together all four, together with *A. minimus*, clade with strong support (1.00 posterior probability) to the exclusion of all other known species of antechinus (Figs 2-3). Although the two Tasmanian Dusky Antechinus, *A. swainsonii* and *A. vandycki* sp. nov. are clearly resolved as genetic sisters, the relationships between between these taxa, *A. mimetes*, *A. arktos* and *A. minimus* are less clear.

Morphologically, the 4 species (5 taxa) of Dusky Antechinus are clearly allied with, but to the exclusion of, *A. minimus*; the latter is strikingly different in fur colour, body shape (squatter, shorter-tailed) and skull features, compared to all Dusky Antechinus, the various species of which differ distinctly but more subtly to each other as a discrete group. The fact that all members of the Dusky Antechinus complex do not form a discrete *genetic* clade to the exclusion of *A. minimus* speaks to the deep and comparable level of divergence between all Dusky Antechinus (7.5-12.5% between species pairs) and those between each Dusky Antechinus species and the Swamp Antechinus (7.6-12.0%). Moreover, it suggests that collectively, Dusky and Swamp Antechinuses shared a common ancestor sometime in the past.

Thus, based on comparative genetic and morphological (external colour and craniodental) differences, we have nominated two new species of antechinus as part of the *A. swainsonii* complex. The total recognised species in the complex shifts from two (*A. arktos*, *A. swainsonii*) as listed by Baker *et al.*, (2014) to four (refer Fig.20), presented here, thus: first, the Black-tailed Dusky Antechinus, *A. arktos* Baker, Mutton, Hines & Van Dyck; second, the Mainland Dusky Antechinus *A. mimetes* (Thomas) two subsp. raised, the nominate *A. m. mimetes* (Thomas) subsp. raised and secondarily *A. m. insulanus* Davison subsp. transferred; third, the Tasmanian Dusky Antechinus *A. swainsonii* (Waterhouse); fourth, the Tasman Peninsula Dusky Antechinus *A. vandycki* sp. nov.

Of species pairs within the Dusky Antechinus group, *A. swainsonii* and *A. vandycki* sp. nov. are closest genetically (and morphologically), ranging from 7.3-8.6% divergence at mtDNA. Comparatively, this is larger than the mtDNA divergence at some species pairs already named in the genus, such as *A. stuartii* / *A. subtropicus* (5%) and *A. leo* / *A. adustus* (5.4 – 6.9%). It is telling that from samples in our collection of *A. swainsonii* across Tasmania, ranging from Arthur River in the north to Bruny Island in the south, some 300 km straight-line distance, the genetic difference ranges from just 0 - 3.3%. And comparatively, for samples of *A. swainsonii* near Hobart to those of *A. vandycki* sp. nov. on Tasman Peninsula, a mere 40 km straight-line distance, the pairwise genetic difference is a striking 8% (refer Fig. 21). All 6 male *A. vandycki* sp. nov. captured in our surveys (3 sites across about 10 km maximum linear distance) were sequenced at mtDNA and represented in total 2 different genetic haplotypes, just 2 bases divergent to each other (about 0.4%).

Another interesting genetic pattern recovered here is that between the two subspecies of *A. mimetes*. *Antechinus m. mimetes* (Vic, NSW) and *A. m. insulanus* (Grampians NP, Vic) range from 2.0 - 4.3% divergent at mtDNA, with samples of the two subspecies in some cases less than 100 km apart geographically. In contrast, *A. m. mimetes* across its considerable geographic range from Cape Otway in southern Victoria to Ebor in north-east NSW, some 1,000 km straight-line distance, is just 0 - 4.1% (refer Fig.21). Notably, the two subspecies strongly clade together as part of the *A. mimetes* species clade to the exclusion of all other species, but the range of genetic divergence and (in particular) striking

TABLE 5. Univariate statistics: means, standard deviations and range minima and maxima of measured variables for *Antechinus arktos*.

MALES						FEMALES					
	Valid N	Mean	Min	Max	St. Dev.		Valid N	Mean	Min	Max	St. Dev.
wt	2	89.85	59.70	120.00	42.64	wt	1	46.30	46.30	46.30	na
hb	5	131.53	108.58	145.00	14.91	hb	3	108.89	106.22	111.20	2.51
tv	6	118.01	100.42	131.00	14.22	tv	3	99.12	94.20	106.88	6.80
hf	6	23.27	21.88	24.00	0.80	hf	3	21.43	20.00	22.20	1.24
e	6	17.15	15.47	19.00	1.39	e	3	16.70	16.10	17.72	0.89
APV	6	4.76	4.52	5.05	0.22	APV	3	4.45	4.31	4.64	0.17
BL	6	32.44	30.45	33.75	1.55	BL	3	29.54	29.12	30.14	0.53
Dent	6	26.31	24.63	27.41	1.16	Dent	3	24.30	24.14	24.51	0.19
IBW	6	5.08	4.93	5.23	0.13	IBW	3	4.68	4.53	4.83	0.15
IOW	6	8.05	7.87	8.51	0.24	IOW	3	7.94	7.78	8.13	0.18
IPV	6	4.11	3.97	4.24	0.12	IPV	3	4.05	3.94	4.13	0.10
M^{2}W	6	2.41	2.35	2.52	0.06	M^{2}W	3	2.40	2.35	2.43	0.04
NW	6	3.15	2.99	3.43	0.16	NW	3	2.90	2.76	3.02	0.13
OBW	6	13.21	12.63	13.72	0.41	OBW	3	12.38	12.32	12.46	0.07
PPV	6	5.85	5.02	6.52	0.57	PPV	3	5.56	5.45	5.76	0.17
R-LC^1	6	5.10	4.93	5.31	0.16	R-LC^1	3	4.68	4.62	4.72	0.05
R-LM^1	6	9.57	9.12	9.90	0.29	R-LM^1	3	8.74	8.66	8.79	0.07
R-LM^{1}T	6	8.15	7.97	8.29	0.14	R-LM^{1}T	3	7.77	7.71	7.82	0.06
R-LM^2	6	11.42	10.95	11.65	0.27	R-LM^2	3	10.60	10.51	10.68	0.09
R-LM^3	6	14.09	13.55	14.70	0.42	R-LM^3	3	13.29	13.01	13.47	0.25
ZW	6	18.27	16.65	19.22	1.20	ZW	3	16.61	16.27	17.10	0.43
HT	6	10.95	10.55	11.38	0.27	HT	3	10.60	10.56	10.64	0.04
PL	6	18.38	17.45	19.04	0.61	PL	3	17.45	17.26	17.71	0.23
SWR-LC^{1}B	6	4.60	4.33	5.03	0.25	SWR-LC^{1}B	3	4.09	4.03	4.13	0.05
TC	6	3.22	2.97	3.38	0.15	TC	3	3.14	3.03	3.33	0.17
NWR	6	5.75	5.22	6.17	0.37	NWR	3	4.99	4.82	5.32	0.29
PML	6	10.23	9.68	10.78	0.44	PML	3	9.57	9.37	9.85	0.25
UML	6	7.35	7.21	7.55	0.11	UML	3	7.33	7.19	7.46	0.14
HT-B	6	8.76	8.53	9.08	0.20	HT-B	3	8.35	8.10	8.48	0.22
BuL	6	4.57	4.25	4.79	0.21	BuL	3	4.48	4.37	4.55	0.09
I^1-P^3	6	10.03	9.58	10.29	0.26	I^1-P^3	3	9.48	9.32	9.66	0.17
LML	6	7.83	7.72	8.07	0.12	LML	3	7.74	7.57	7.92	0.18
I$_1$-P$_3$	6	7.99	7.16	8.36	0.44	I$_1$-P$_3$	3	7.35	6.98	7.68	0.35
M$_2$W	6	2.27	2.13	2.35	0.08	M$_2$W	3	2.28	2.20	2.35	0.08
UPL	6	4.50	4.29	4.71	0.17	UPL	3	4.15	3.99	4.24	0.14

TABLE 6. ANOVA F-statistics (top two lines) for variation at each of the measured variables among all antechinus species and subspecies. Subsequent rows show significance values for ANOVA Post-Hoc tests of *Antechinus swainsonii* paired with each of its 14 congeners, for each measured variable. Shaded cells are significant at p=0.05, unshaded cells are not significant.

Comparison	sex	wt	hb	tv	hf	e	APV	BL	Dent	IBW	IOW	IPV	M^{2}W	NW	OBW	PPV	R-LC^1	R-LM^1	R-LM^{1}T
ANOVA F - all species	M	29.79	31.94	37.56	54.70	20.38	250.20	49.18	55.08	41.20	85.62	93.02	52.06	32.10	26.51	24.30	56.37	48.79	31.50
ANOVA F - all species	F	30.72	25.77	25.00	30.13	19.22	222.60	51.41	70.84	40.82	97.85	76.72	47.44	19.70	28.79	19.15	43.34	44.27	26.97
A. vandycki	M	1.00	0.80	0.64	1.00	1.00	0.00	0.59	0.41	1.00	1.00	0.04	1.00	1.00	0.98	0.04	0.98	1.00	0.99
A. mimetes mimetes	M	1.00	0.54	1.00	1.00	1.00	0.00	1.00	1.00	0.64	0.95	0.00	0.87	0.15	1.00	1.00	1.00	0.38	1.00
A. mimetes mimetes	F	1.00	0.26	0.99	1.00	1.00	0.00	1.00	1.00	0.98	1.00	0.00	1.00	1.00	1.00	0.85	1.00	1.00	1.00
A. mimetes insulanus	M	1.00	1.00	0.22	1.00	1.00	0.00	0.04	0.03	0.00	1.00	0.00	0.00	0.00	0.00	1.00	0.61	0.66	0.03
A. mimetes insulanus	F	0.87	1.00	0.17	0.88	0.33	0.00	0.08	0.01	0.00	1.00	0.00	0.00	0.00	0.00	0.85	0.05	1.00	0.00
A. arktos	M	0.86	1.00	0.00	0.78	1.00	0.00	0.07	0.12	0.01	1.00	0.00	0.56	0.00	0.03	0.77	0.14	0.00	0.25
A. arktos	F	1.00	1.00	0.68	0.56	0.98	0.00	1.00	0.90	0.82	1.00	0.00	0.39	0.19	0.84	0.93	0.75	1.00	0.90
A. minimus	M	0.72	0.14	0.00	0.00	0.15	0.00	0.13	0.02	1.00	0.00	0.00	1.00	0.87	1.00	0.99	0.04	0.02	0.75
A. minimus	F	0.42	0.39	0.00	0.02	0.54	0.00	0.00	0.00	1.00	0.00	0.00	1.00	0.06	1.00	1.00	0.00	0.02	1.00
A. adustus	M	0.00	0.00	1.00	0.00	0.61	0.00	0.00	0.00	1.00	0.00	0.00	0.17	0.74	0.48	0.94	0.00	0.76	1.00
A. adustus	F	0.00	0.00	1.00	1.00	1.00	0.00	0.00	0.00	0.99	0.00	0.00	0.09	0.76	0.00	0.82	0.00	1.00	0.99
A. agilis	M	0.00	0.00	1.00	0.00	0.32	0.00	0.00	0.00	0.00	0.00	0.00	0.31	0.34	0.00	0.00	0.88	1.00	0.21
A. agilis	F	0.00	0.00	1.00	0.00	1.00	0.00	0.00	0.00	0.00	0.00	0.00	1.00	1.00	0.00	0.01	0.02	0.90	1.00
A. argentus	M	0.07	0.00	1.00	0.00	1.00	0.00	0.00	0.00	0.14	0.00	0.00	1.00	0.75	1.00	0.12	0.02	0.02	0.99
A. argentus	F	0.00	0.00	1.00	0.04	1.00	0.00	0.00	0.00	0.06	0.00	0.00	1.00	0.96	0.87	0.01	0.70	0.91	1.00
A. bellus	M	1.00	1.00	0.00	1.00	0.00	0.00	1.00	1.00	0.00	0.00	0.00	0.00	0.00	0.00	0.00	0.00	0.00	0.00
A. bellus	F	0.00	0.63	0.00	0.89	0.00	0.00	0.41	0.03	0.00	0.00	0.00	0.00	0.00	0.00	0.00	0.00	0.00	0.00
A. flavipes flavipes	M	0.51	0.00	0.97	0.00	1.00	0.00	0.00	0.00	0.00	0.00	0.00	0.00	0.00	0.09	0.00	0.00	0.00	0.00
A. flavipes flavipes	F	0.06	0.00	0.53	0.00	1.00	0.00	0.00	0.00	0.00	0.00	0.00	0.00	0.00	1.00	0.00	0.00	0.00	0.00
A. flavipes leucogaster	M	0.01	0.00	0.30	0.00	1.00	0.00	0.00	0.00	0.00	0.00	0.00	0.1.0	0.00	0.67	0.00	0.00	0.00	0.00
A. flavipes leucogaster	F	0.00	0.00	0.00	0.00	0.99	0.00	0.00	0.00	0.00	0.00	0.00	0.00	0.00	1.00	0.00	0.00	0.00	0.02
A. flavipes rubeculus	M	1.00	0.78	1.00	1.00	1.00	0.00	1.00	0.81	1.00	0.00	0.00	0.00	0.00	0.00	0.25	0.00	0.00	0.00
A. flavipes rubeculus	F	1.00	1.00	1.00	1.00	1.00	0.00	1.00	0.90	1.00	0.00	0.00	0.00	0.00	0.00	0.04	0.00	0.00	0.00
A. godmani	M	0.00	1.00	0.00	0.39	0.17	0.00	0.00	0.00	0.00	1.00	0.00	0.00	0.90	0.00	1.00	0.00	0.00	0.00
A. godmani	F	0.00	1.00	0.00	0.59	0.00	0.00	0.02	0.09	0.00	0.99	0.00	0.00	1.00	0.00	1.00	0.00	0.00	0.00
A. leo	M	0.16	1.00	0.00	0.00	0.01	0.00	0.14	0.66	0.00	0.00	0.00	0.00	0.00	0.00	1.00	0.00	0.00	0.00
A. leo	F	1.00	1.00	0.01	0.00	0.00	0.00	1.00	1.00	0.00	0.00	0.00	0.00	0.00	0.00	1.00	0.00	0.00	0.00
A. mysticus	M	0.08	0.00	1.00	0.00	1.00	0.00	0.00	0.00	0.00	0.00	0.00	0.01	0.38	1.00	0.92	0.00	0.00	0.05
A. mysticus	F	0.00	0.00	1.00	0.00	0.92	0.00	0.00	0.00	0.00	0.00	0.00	0.02	0.69	0.84	0.99	0.00	0.08	0.20
A. stuartii	M	0.00	0.00	0.99	0.00	1.00	0.00	0.00	0.00	0.00	0.00	0.00	0.96	0.25	0.26	1.00	0.02	1.00	1.00
A. stuartii	F	0.00	0.00	0.21	0.00	1.00	0.00	0.00	0.00	0.00	0.00	0.00	0.86	1.00	0.00	0.82	0.00	1.00	1.00
A. subtropicus	M	0.93	0.06	1.00	0.00	1.00	0.00	0.00	0.00	0.44	0.00	1.00	0.00	0.12	1.00	0.00	0.00	0.09	0.72
A. subtropicus	F	0.05	0.00	1.00	0.12	1.00	0.00	0.00	0.00	0.52	0.00	1.00	0.00	0.16	0.98	0.00	0.00	1.00	0.59

TABLLE 6. continued …

Comparison	sex	R-LM^2	R-LM^3	ZW	HT	PL	SWR-LC^{1}B	TC	NWR	PML	UML	HT-B	BuL	I1-P^3	LML	I_1-P_3	M_2W	UPL
ANOVA F - all species	M	49.52	30.88	18.67	37.40	71.93	44.90	27.15	14.90	20.66	57.00	39.00	24.89	87.10	56.54	130.45	34.96	101.34
ANOVA F - all species	F	48.30	29.58	20.39	52.18	79.90	37.71	31.92	14.70	28.47	58.75	58.78	24.47	46.78	62.14	126.25	47.89	95.59
A. vandycki	M	1.00	1.00	1.00	1.00	0.28	0.99	1.00	1.00	1.00	1.00	1.00	0.92	0.34	1.00	0.22	1.00	0.74
A. mimetes mimetes	M	1.00	0.70	1.00	0.91	0.99	1.00	0.00	0.46	1.00	1.00	0.73	1.00	0.50	1.00	0.96	1.00	1.00
A. mimetes mimetes	F	1.00	0.15	1.00	0.72	0.99	1.00	0.48	1.00	1.00	1.00	1.00	1.00	0.76	1.00	0.50	0.94	1.00
A. mimetes insulanus	M	1.00	0.02	0.00	0.07	0.22	0.73	0.00	0.02	0.00	0.00	0.02	0.89	1.00	0.00	0.73	0.04	1.00
A. mimetes insulanus	F	1.00	0.00	0.00	0.00	0.07	0.13	0.00	0.01	0.00	0.00	0.76	0.21	1.00	0.00	1.00	0.00	1.00
A. arktos	M	0.13	0.02	0.10	0.75	0.98	0.12	0.00	0.00	0.11	0.01	0.46	0.16	1.00	0.82	1.00	0.99	1.00
A. arktos	F	0.99	0.47	0.89	0.79	1.00	0.98	0.09	0.26	0.38	0.00	1.00	0.14	1.00	0.43	1.00	0.06	1.00
A. minimus	M	0.07	0.21	1.00	1.00	0.00	0.13	0.57	1.00	1.00	0.01	1.00	1.00	0.00	0.00	0.00	0.66	0.00
A. minimus	F	0.02	0.21	1.00	0.99	0.00	0.00	1.00	0.17	0.48	0.00	1.00	1.00	0.00	0.00	0.00	1.00	0.00
A. adustus	M	0.53	1.00	1.00	0.00	0.00	0.01	0.79	0.26	0.00	0.00	0.00	0.11	0.00	0.00	0.00	1.00	0.00
A. adustus	F	0.99	1.00	0.99	0.00	0.00	0.00	0.98	0.07	0.00	0.00	0.00	0.00	0.00	0.00	0.00	0.14	0.00
A. agilis	M	0.90	1.00	0.50	0.00	0.00	0.96	1.00	0.35	0.00	0.00	0.00	0.93	0.00	0.00	0.00	0.00	0.00
A. agilis	F	0.00	0.13	1.00	0.00	0.00	0.02	1.00	0.04	0.00	0.00	0.00	1.00	0.00	0.00	0.00	1.00	0.00
A. argentus	M	0.00	0.04	1.00	0.00	0.00	0.02	1.00	1.00	0.98	0.21	0.00	1.00	0.00	0.03	0.00	1.00	0.00
A. argentus	F	0.72	0.68	1.00	0.00	0.00	0.73	1.00	0.86	0.07	0.15	0.00	1.00	0.00	0.07	0.00	1.00	0.00
A. bellus	M	0.00	0.00	0.00	1.00	0.59	0.00	1.00	1.00	1.00	0.87	0.11	0.00	0.00	0.99	0.00	0.00	0.00
A. bellus	F	0.00	0.00	0.00	1.00	0.00	0.00	0.71	0.99	0.56	0.03	0.00	0.00	0.00	0.01	0.00	0.00	0.00
A. flavipes flavipes	M	0.00	0.00	0.06	0.01	0.00	0.00	1.00	1.00	0.39	1.00	0.00	0.00	0.00	1.00	0.00	0.00	0.00
A. flavipes flavipes	F	0.00	0.00	0.54	0.00	0.00	0.00	0.14	0.67	0.00	0.97	0.00	0.00	0.00	1.00	0.00	0.00	0.00
A. flavipes leucogaster	M	0.00	0.00	0.20	0.02	0.00	0.00	0.99	1.00	0.14	0.00	0.00	0.00	0.00	0.00	0.00	1.00	0.00
A. flavipes leucogaster	F	0.00	0.00	0.73	0.00	0.00	0.00	1.00	0.84	0.00	0.00	0.00	0.04	0.00	0.00	0.00	0.00	0.00
A. flavipes rubeculus	M	0.00	0.00	0.00	0.93	0.26	0.00	1.00	0.04	0.89	0.02	0.32	0.00	0.00	0.35	0.00	0.00	0.00
A. flavipes rubeculus	F	0.00	0.00	0.00	0.99	0.02	0.00	1.00	0.99	1.00	0.00	0.00	0.00	0.00	0.00	0.00	0.00	0.00
A. godmani	M	0.00	0.00	0.00	0.86	0.00	0.00	0.00	0.08	1.00	0.00	1.00	0.91	1.00	0.00	0.00	0.00	1.00
A. godmani	F	0.00	0.00	0.00	1.00	0.06	0.00	0.00	0.94	0.98	0.00	0.91	0.88	1.00	0.00	0.00	0.00	1.00
A. leo	M	0.00	0.00	0.00	1.00	1.00	0.00	0.00	0.00	0.00	0.00	0.99	0.00	0.00	0.00	0.00	0.00	0.00
A. leo	F	0.00	0.00	0.00	1.00	1.00	0.00	0.00	0.01	0.30	0.00	0.00	0.00	0.00	0.00	0.00	0.00	0.00
A. mysticus	M	0.00	0.00	0.94	0.00	0.00	0.00	1.00	1.00	0.66	0.00	0.00	0.28	0.00	0.00	0.00	1.00	0.00
A. mysticus	F	0.00	0.00	1.00	0.00	0.00	0.00	1.00	1.00	0.00	0.00	0.00	0.65	0.00	0.00	0.00	1.00	0.00
A. stuartii	M	1.00	1.00	0.95	0.00	0.00	0.02	0.75	1.00	0.00	0.00	0.00	1.00	0.00	0.00	0.00	1.00	0.00
A. stuartii	F	1.00	1.00	0.32	0.00	0.00	0.00	1.00	0.02	0.00	0.00	0.00	1.00	0.00	0.00	0.00	0.97	0.00
A. subtropicus	M	0.51	0.95	1.00	0.00	0.00	0.00	0.00	1.00	0.61	0.43	0.00	1.00	0.00	0.00	0.00	1.00	0.00
A. subtropicus	F	0.99	0.99	1.00	0.00	0.00	0.00	1.00	1.00	0.45	0.39	0.00	1.00	0.00	0.08	0.00	0.00	0.00

morphological differences between the two subspecies (*A. m. insulanus* have larger, broader skulls) is also clearcut. It is also interesting that both *A. m. insulanus* and *A. agilis* from the Grampians are both genetically and morphologically different to respective *A. m. mimetes* and *A. agilis* from surrounding areas in Victoria immediately outside the Grampians – this suggests a common history of geographical isolation for antechinus within Grampians NP. Comparatively, Crowther (2002) also noted the larger size of *A. agilis* from the Grampians, while Davison (1991) noted the relatively larger size of *Grampians A. swainsonii* from conspecifics, on the strength of which he raised the then *A. swainsonii insulanus* (now *A. mimetes insulanus).*

For clarity, common names of the four species are proposed here as variants of 'Dusky Antechinus'. This necessitates a proposed common name change for *A. arktos* from our previous (Baker *et al.* 2014) 'Black-tailed Antechinus' to '*Black-tailed Dusky Antechinus*'. At the time of naming *A. arktos*, we were unaware of further variation within *A. swainsonii*; but given the suite of species now reported, retaining the original epithet nested within the common name of *A. arktos* seems most appropriate.

The *Anetchinus swainsonii* from Tasmania named by Waterhouse in 1840 from a specimen in the private collection of William Swainson by primacy retains the original specific designator. Subsequently, Captain Wilkins collected an animal from Guy Fawkes district, near Ebor in north-east NSW, named by legendary BMNH taxonomist Oldfield Thomas in 1924 as the subspecies *A. swainsonii mimetes* (although then under genus *Phascogale*). Based on our reported striking genetic (on average 10% divergent at Cytb mtDNA) and morphological differences of *A. swainsonii mimetes* with both Tasmanian species, coupled with their separation in allopatry, we have raised Thomas' subspecies *mimetes* to full species status, thus *A. mimetes*. Davison (in 1991) had nominated another subspecies of mainland *swainsonii* to account for larger animals from Grampians NP (Vic), his *A. s. insulanus*. We find that *insulanus* is a variant lying within the newly raised species *mimetes* based on both shallow but distinctive genetic variation and clear craniodental variation. Thus, we have designated by primacy Thomas' Guy Fawkes animals *Antechinus mimetes mimetes* and secondarily Davison's Grampians animals are transferred to *Antechinus mimetes insulanus*. Other than *A. m. insulanus* from the Grampians, all other *swainsonii* complex individuals sampled from the Australian mainland between southern Victoria and Guy Fawkes (in north-east NSW) are apparently *A. m. mimetes* based on both morphology (see species by species differences in Results) and genetics (Figs 2-3 and AMB and TYM unpublished data).

To our knowledge, prior to the present study, there was only one collected voucher specimen of *A. vandycki*: sp. nov. This was obtained by John Gould (no date), held in the British Museum of Natural History, and registered there as a male *A. swainsonii*. Although no genetic data could be obtained for this specimen, morphologically it was clearly very similar to the six male *A. vandycki* sp. nov. that were included here and different to the suite of *A. swainsonii* from elsewhere in Tasmania.

All four species (and 5 taxa) within the *swainsonii* complex are distinctive morphologically. As one moves from south (higher latitudes) to north (lower latitudes) the fur colour generally changes from predominantly greyish (*vandycki* sp. nov. and *swainsonii*), to more predominantly brownish (*mimetes*) to predominantly brownish with more russet rump (*arktos*). Tail and hindfoot colour also predominantly darkens from southern (greyish/brown) to northern latitudes (through brown, dark brown, to black). The skull becomes generally stouter / broader from *swainsonii* through *mimetes mimetes* to *arktos/mimetes insulanus*. However, *vandycki* sp. nov. skulls are somewhat more robust than *swainsonii*; the latter are the most delicate of the group. Generally speaking, the length of the front holes in the skull palate (APV) and the distance between the front and back palate holes (IPV) are good diagnostics to separate the four species craniodentally; the front palate holes are very large indeed in *vandycki* sp. nov. and neatly separate this new animal from every other antechinus species. The front palate holes become smaller as one moves through each

Dusky Antechinus species, going northwards (*swainsonii*, *mimetes*, *arktos*); the functionality of these craniodental differences (if, indeed, any exists) remain a mystery.

Biogeography

Resolving *Antechinus* phylogeography using genetic and fossil dating was not the aim of the present study; TYM's PhD, nearing completion, and incorporating a great many more mtDNA and nuclear sequences, will focus on this important task. However, it is worth discussing a few salient features of our phylogenetic tree as they may relate to biogeographic processes affecting the Dusky Antechinus complex. The genetic differences among (and relative to congeners, within) all members of the Dusky Antechinus complex are strikingly deep, suggesting this species group may be prone to geographic isolation. Certainly, their general preference for well-forested, high, cold and wet habitat types (Baker *et al.* 2014) may predispose the group to such isolating forces over time, especially as Australia has become drier and less-forested over time. The deep structuring between each of the two Tasmanian species (*A. swainsonii* and *A. vandycki* sp. nov) and proximate mainland *A. mimetes* is particularly striking. Such deep divergences strongly suggest that speciation between these forms occurred well before separation of Tasmania from mainland Australia (regardless of which date for Tasmanian/mainland separation one ascribes to). Under one plausible scenario, even hundreds of thousands of years before continental separation, conditions may have favoured geographic isolation of some ancestral forms of this dasyurid complex and over time genetic isolation has conceivably resulted in their speciation; subsequently, Tasmania became separated from continental Australia, presumably carrying these already distinct taxa with it. Similar scenarios have been proposed to explain striking genetic divergences between Tasmanian and Victorian forms of the Tiger Quoll (*Dasyurus maculatus*; Firestone *et al.* 1999) and also the recently discovered deep divergences between mainland and Tasmanian forms of our iconic monotreme, the Platypus (*Ornithorhynchus anatinus*; Gongora *et al.*, 2012).

The comparative biogeography of the three Tasmanian species of antechinus, *A. swainsonii, A. vandycki* sp. nov. and *A. minimus*, is also intriguing. It is plausible that *A. vandycki* sp. nov. has been isolated in the past by unsuitable habitat across the East Bay Neck between Dunalley and Blackman Bay (on Forestier Peninsula) and also further to the south at Eaglehawk Neck (Tasman Peninsula). In the latter location, the 200 metre long isthmus is so narrow that ferocious wild dogs and a handful of military guards were able to prevent escaped convicts from Port Arthur gaining safe passage north onto Tasmania proper some 150 years ago. *Antechinus vandycki* sp. nov. has been perhaps just as effectively confined to Tasman Peninsula over deeper time by geomorphology alone.

Interestingly, our research group have also caught *A. minimus* with *A. vandycki* sp. nov. on Fortescue Bay (at low altitude, 50 m), the southernmost capture site on Tasman Peninsula; *A. minimus* from there is genetically similar to *A. minimus* from other locations on Tasmania (data not shown). So, if these narrow necks of land have played a part in isolating *A. swainsonii* from *A. vandycki* sp. nov. then they have apparently not isolated the *A. minimus* population from conspecifics as effectively or for as long. This may at least partly be explained by their respective habitat preferences, because while members of the Dusky Antechinus complex typically prefer closed, wet, higher altitude forest (Baker *et al.* 2014; Dickman 2008), Swamp Antechinuses are more commonly found in lower altitude, more open habitat, as their name suggests (Gibson *et al.* 2004; Sale *et al.* 2006; Wilson & Bachmann 2008; Wilson *et al.*, 2001). Interestingly, *A. swainsonii* from South Bruny Island, which today is separated from mainland Tasmania, are only slightly different genetically (1-2%) from other *A. swainsonii* on southern Tasmania (Southwest NP and Mount Wellington). So whatever factors explain the evolutionary history of these antechinus species on Tasmania, it is not as simple as invoking isolation due to obvious geographic

FIG. 19. (A-C) Habitat photographs of the *A. vandycki* sp. nov. holotype locality – Lichen Road, Tasman Peninsula, Tasmania. Photographs by Eugene Mason (QUT).

barriers. At present, unfortunately we know little about *A. swainsonii*, especially in south-east Tasmania, and less still of *A. vandycki*. sp. nov. Our research group aims to spend the next few years further investigatng the comparative biology of the species.

Ecology

Generally speaking, catchability of all four species in the Dusky Antechinus complex is low. Typically, even during late Autumn/winter during pre-mating activity (optimum catchability) rarely is the catching rate higher than one every 200 trap/nights, although there are exceptions, such as some populations of *A. mimetes mimetes* (see e.g. Dickman 1986a, b; 1988a, b). For antechinus that probably spend much or most of the time foraging on the ground (Dickman, 1986a, b; 1988 a, b; 2008) (cf. their mostly semi-arboreal congeners, Baker *et al.*, 2014), this is in one sense a surprisingly low capture rate given that antechinus are typically captured in Elliott traps deployed on the ground. Because of this, it has been supposed that low catchability of Dusky Antechinus is best explained by their trap-shyness. This is certainly plausible. However, in the course of the present work we have done a lot of trapping of the various species within the Dusky Antechinus complex and in numerous cases have recaught the same individuals across successive trap/nights, so there seems at least to be little reticence from the animals to re-enter traps after capture, if they are initially overly suspicious. Dusky Antechinus complex species are large antechinus (some males may even approach 200g) and if they are largely limited to the ground they may require relatively large home ranges to access food resources. Thus, in any given trapping grid, one may be less likely to catch such species that support a lower density of individuals. So low densities where Dusky Antechinus occur, especially as one moves north through NSW and into Qld where habitat requirements (high, cold, wet) are less often satisfied, may at least in part explain their characteristically low capture rates in many trapping surveys in those places. One of us (ELG) will be testing this idea with *A. arktos*, where they co-occur (apparently in low abundance) with a plethora of *A. stuartii* (regularly one *A. stuartii* captured in every 4-5 traps deployed) in Springbrook NP, using a combination of radio-tracking and baited remote RFID (Radio Frequency IDentification) camera stations (where already

FIG. 20. Live photos of the four species in the Dusky Antechinus Species complex. Clockwise from top left: *Antechinus vandycki* sp. nov. (male, HOLOTYPE, QM JM 20111), *A. swainsonii* (male, general collection, QM JM 20107), *A. arktos* (male, PARATYPE, QM JM 20010), *A. mimetes* (female, general collection, QM JM 20112). Photographs by Gary Cranitch (QM).

pit-tagged individuals are recorded on each visit to the station). This data may indicate comparative home range size and over time hopefully relative abundance of each species using combined Elliott-trapping and remote cameras (the latter can be left in the field for a month at a time constantly recording data).

With respect to habitat requirements, *A. swainsonii* occurs in a range of forested habitats in Tasmania. Dominant species include: *Nothofagus cunninghamii, Atherosperma moschatum, Eucryphia lucida, Phyllocladus rhomboidalis* and *Anodopetalum biglandulosum*. In fire-affected areas, where the species is found, landscapes may be dominated by: *Eucalyptus* spp., understorey plants including *Olearia argyrophylla, Pittosporum bicolor, Drimys lanceolata, Persoonia gunnii, Anopterus glandulosa* and *Dicksonia antarctica*. Ecotonal regrowth habitats occupied by *A. swainsonii* are typically characterised by: *Ghania trifida, Sprengelia incarnata, Epacris gunnii, Monotoca* sp., *Boronia rhomboidea, Leptospermum* sp., *Gleichenia alpina, Casuarina dystyla, Eucalyptus gunnii, Poa caespitosa, Calorophus lateriflorus, Restio australis* and *Lepidosperma filiforme*. Throughout the range of this species, rainfall may be in excess of 250 cm p.a. and temperatures may vary from as low as -12°C in subalpine habitat to 35°C in coastal areas; here, *A. swainsonii* is regularly found to occupy areas of dense cover and thick litter and is not trapped in treeless expanses of button grass (*Mesomelaena sphaerocephala*), where it is often replaced by *A. minimus* (Dickman 2008; Green 1972; Menkhorst 1995; Sanecki *et al.* 2006; Williams & Williams 1982).

The *Antechinus vandycki* sp. nov. type locality at Lichen Road on Tasman Peninsula features wet sclerophyll temperate rainforest with many fallen logs and a dense understorey. Floristically, the area is typical of Tasmanian temperate

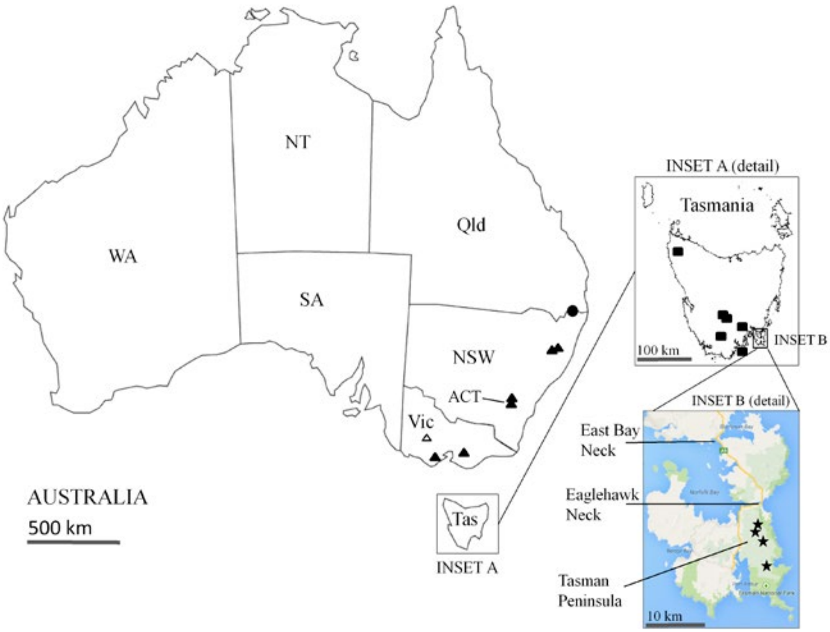

FIG. 21. Relative geographic distributions of Dusky Antechinus species, showing locations where combined genetic and morphological data was obtained from various individuals (*Antechinus arktos* [Qld] closed circle; *A. mimetes mimetes* closed triangles [NSW, ACT, Vic]; *A. mimetes insulanus* [Vic] open triangle; *A. swainsonii* [Tas, INSET A] closed squares; *A. vandycki* sp. nov. [Tasman Peninsula, Tas, INSET B] closed stars).

rainforest, but there are only limited stands existent on Tasman Peninsula, which in many places has already been cleared, is under plantation or has been fire-affected. The holotype locality featured Native Laurel, *Anopterus glandulosa*, with *Eucalyptus delegatensis* and *Eucalyptus obliqua* and an understorey of *Blechnum nudum*. In a study of mammalian predator and prey interactions and their responses to a range of predator odour cues, Lazenby & Dickman (2013) reported vegetation structure at one site on Tasman Peninsula which contained *A. vandycki* sp. nov. (that we have genetically confirmed). This site is roughly 1.5 km straight-line distance to the south of the *A. vandycki* sp. nov. holotype locality, and described generically by Lazenby and Dickman as cool temperate wet forest containing emergent eucalypts over rainforest/scrub communities, typically featuring *Nothofagus*, *Atherosperma*, *Eucryphia* and *Athrotaxis*.

Antechinus mimetes in Victorian populations is largely restricted to dense vegetation in damp environments (>800 mm rainfall per annum) at altitudes from sea level to over 1,800 m, where vegetation types include alpine heath, woodland, high and low altitude rainforest, *Banksia* woodland and wet heath. In New South Wales, the subspecies is found on and east of the Great Dividing Range in wet sclerophyll and rainforest gullies, heathlands, coastal sand dunes and swamps, as well as sub-alpine woodland with dense shrubby understorey (Dickman 2008; Lunney *et al.* 2001; Menkhorst 1995; Williams & Williams 1982).

Antechinus arktos favours the highest altitude (>800 m), wettest, coldest patches of rainforest in the Tweed Volcano Caldera. The type locality at Best of All Lookout (Springbrook NP) featured complex notophyll vine forest in areas featuring moderately steep, bouldery headwater gully with Stream Lily, *Helmholtzia glaberrima,* and Antarctic Beech, *Nothofagus moorei* prominent

(Baker *et al.* 2014). This antechinus species was historically found in mountain mallee heath, approximately 162 ha in size, on rhyolitic soils, in the Dave's Creek area of Lamington National Park (28°13´S, 153°13´E, 840 m altitude). The area was surrounded by rainforest and wet sclerophyll forest. A prominent trachyte dyke known as Surprise Rock outcrops from nearby the capture site. Plant species present at this site included: *Leptospermum lanigerum* (now *L. trinervium*), *L. flavescens* (now *L. polygalifolium*), Banksia collina (now *B. neoanglica*), *Leucopogon melaleucoides*, *Callistemon montanus* (now *Melaleuca montana*), *Lepidosperma canescens* (now *L. clipeicola*) and the mallee *Eucalyptus codonocarpa* (Baker *et al.* 2014; Van Dyck & Ogilvie 1977).

Breeding ecology is little known for most members of the Dusky Antechinus complex. Mating timing in the group seems to range from May – September for *A. mimetes mimetes* (with coastal and low altitude populations breeding earliest; Williams & Williams 1982), May-June for *A. mimetes insulanus* (Davison 1991), September - October for *A. swainsonii* (Green 1972; AMB, pers. obs.), most likely mid-late September for *A. arktos* (ELG pers. obs.); there is no reliable information for breeding timing in *A. vandycki* sp. nov. although it is worth noting that a 92g adult male was caught by us at Lichen Road on Tasman Peninsula in early May 2014, suggesting an animal more than six months old which points towards an early November birth, at latest, the year before. Moreover, in the course of her PhD work, Lazenby (pers. comm.) caught three males between 8 and 12 March, 2011 that ranged from 60-65 g, which is also suggestive of adult animal size. Based on this (admittedly scant) data, and coupled with the notion that higher latitude populations of *A. swainsonii* tend to breed later (Dickman 1982; Williams & Williams 1982; McAllan 2003; McAllan *et al.*, 2006), one might guess that timing of breeding in *A. vandycki* sp. nov. is similar to that in *A. swainsonii* and *A. arktos* (Sep–Oct), or if not, slightly earlier (Aug). But this is sheer speculation until we study this *A. vandycki* sp. nov. population between July and October, where its breeding timing secrets will be revealed in short order – this work is currently being planned.

Interestingly, in their investigation of mating timing across the genus *Antechinus*, McAllan *et al.* (2006) found rate of change of photoperiod to be the most important cue in most species. *Antechinus swainsonii* and *A. minimus* were an exception, being more variable, perhaps indicating a more plastic use of photoperiod to synchronise reproduction. The authors hypothesised that this may be in part attributable to interspecific interactions (*A. swainsonii* in Victoria are dominant to *A. agilis* and thus may be under less pressure to select for a particular rate of change of photoperiod) and in part associated with a more generalist diet (*A. swainsonii* and *A. minimus* eat a wider variety of prey than other antechinus, some of which may be less seasonably variable, thus there is less pressure to predict for insect flushes) (McAllan *et al.* 2006). They also noted the genetic and morphological distinctness of *A. swainsonii* and *A. minimus* compared to congeners, as recognised at the time (see also Armstrong *et al.*, 1998; Baverstock *et al.*, 1982; Krajewski *et al.*, 1997; Van Dyck, 2002). The present study, which reaffirms such distinctness and further suggests species level differences between Tasmanian and Victorian *A. swainsonii*, may also help to explain the variability in photoperiod response reported by McAllan *et al.* (2006), where they found mating at comparatively longer absolute photoperiod and ovulation at larger rate of change of photoperiod in Tasmanian versus mainland (Victorian and New South Wales) *A. swainsonii*. It is plausible that some aspects of speciation in the Dusky Antechinus complex may be associated with these variable responses to photoperiod.

Nipple count in females of the Dusky Antechinus complex ranges from 6-10 (Dickman 2008), with the typical condition being 8. Plausibly, there is a pattern in *A. mimetes* where lowland populations tend to have lower nipple numbers than upland populations (Williams & Williams, 1982). One population of *A. mimetes mimetes* studied in Koscuisko NP consistently had females with 10 nipples (Happold 1989, 2011). *Antechinus swainsonii* females tend to have 8 nipples, at least based on several females from different locations examined by AMB that are held in the QVM (Launceston). No female *A. vandycki* sp. nov. have yet been observed in breeding condition, so nipple count and other aspects of female breeding biology in this species are as yet unknown. Our research group are currently investigating comparative breeding ecology and diet of *A. vandycki* sp. nov. and *A. swainsonii*, as part of a proposed PhD project. Preliminary results from ELG's current PhD project on *A. arktos* in Qld suggest that nipple number in this species may be 6.

Distribution & Conservation

Antechinus mimetes mimetes appears widely, if patchily, distributed across numerous sites between southern Victoria and north-east New South Wales (Dickman, 1982, 2008). *Antechinus swainsonii*, similarly, appears widely distributed across Tasmania, particularly in the central northern and western/south-western wilderness areas (AMB, pers. obs. of QVM specimens and data register, M.Dreissen, pers. comm.).

However, *A. vandycki*, sp. nov., *A. arktos* and *A. mimetes insulanus* all appear to be geographically limited (Baker *et al.*, 2014; Davison, 1991; AMB, TYM, EDM, ELG pers. obs.).

Antechinus mimetes insulanus, found only within the confines of Grampians NP in Victoria (Davison 1991), has been regularly caught at several sites across the Park in annual mammal surveys conducted by our colleagues at Deakin over the last few years.

The northern limited *A. arktos* has plausibly retracted to the highest, wettest, coldest reaches of the Tweed Caldera in the face of global warming and may be restricted to just a couple of surviving populations (Springbrook NP, Border Ranges NP), supporting low numbers (Baker *et al.* 2014). This species is the subject of a current PhD project by one of us (ELG) investigating ecology, genetics and distribution. Monthly field surveys in 2014 (between April-October) have returned just 10 individuals (7 males, 3 females) in about 5,000 trap/nights at the Qld type locality (Best of All Lookouts/ Bilborough Ct, Springbrook NP) and 0 individuals in 1,500 trap/nights during a June, 2014 survey from the only known location of the species in NSW (Brindle Creek, Border Ranges NP). *Antechinus arktos* is currently being considered for Endangered species listing under both Qld and NSW state legislation with an application pending for federal EPBC listing.

Despite considerable trapping effort *A. vandycki* sp. nov. is thus far only known, in very low apparent density (6 male [and zero female] captures in 5,000 trap/nights across several field trips in recent years by us), on eastern Tasman Peninsula in a forest block encompassing just 40 km^2. One of three study sites investigated by Lazenby and Dickman (2013) in their camera/capture/release study was on Tasman Peninsula, just 1.5 km south of the *A. vandycki* sp. nov. holotype locality. Between 2009 and 2011, they recorded several captures of *A. vandycki* sp. nov. (one of which has been genetically confirmed by us), including one 45 g female captured on the 16th of May, 2011 (all captures were released). We are currently investigating the ecology, genetics and distribution of *A. vandycki* sp. nov., which will permit us to formally assess status and conservation priorities with state and federal listings both pending. If *A. vandycki* sp. nov. is truly limited to Tasman Peninsula (south of EagleHawk Neck), it will certainly warrant listing in a threatened category because of geographical restriction, small apparent population size and because much of its known (and limited) natural habitat there falls within State Forest and is thus infested with timber plantations (within which the species has been targeted several times and never caught). Throughout the forest block (both intentional and unintentional) fires will also be a conservation concern, if *A. vandycki* sp. nov. behaves like *A. mimetes* in following a secondary succession pattern, typically not moving back into fire-affected / heavily disturbed areas until ten or more years post-disturbance (Dickman, 2008; Lunney *et al.* 2001). Indeed, the fragmented, harvested and fire-affected nature of the Tasman Peninsula forests over the last twenty years may account in part for the very low trapping success for *A. vandycki* sp. nov. (just one male in every 830 trap/nights in our surveys). Another threat to *A. vandycki* sp. nov. (and other native Australian mammalian wildlife) exists in the form of feral cats (*Felis catus*). The Tasmanian Devil (*Sarcophilus harrisii*) population is small on Tasman Peninsula (30-40 disease-free animals, Mike Driessen pers. comm.) and such reduction /removal of a top native predator may result in increased feral cat numbers (Lazenby & Dickman, 2013); cats are common in the east of the Peninsula (often interfering with the Devil trapping program, Mike Driessen, pers. comm.) and will most likely opportunistically prey on *A. vandycki* sp. nov.

Nevertheless, the results of this study have generally positive implications for Tasmanian mammal conservation and tourism, with a new endemic and likely threatened species being identified (*A. vandycki* sp. nov.) and an existing species (*A. swainsonii*) now recognised as apparently endemic to the island. In a small Australian state boasting just six endemic (of 83) mammal species, an increase of two endemic species may prove important, raising its mammalian endemicity rating from 7% to 10%.

ACKNOWLEDGEMENTS

AMB especially wishes to thank his long-time friend and mentor Dr Steve Van Dyck (formerly of QM) for generously sharing his expertise on all things antechinus and making helpful comments on a draft of this work. AMB is also grateful to Harry Hines (QPWS) and Ian Gynther (EHP) for loan of Elliott traps to catch antechinus. This research would not have been possible without the unstinting help of Mike Driessen (DPIPWE), who provided invaluable advice, logistical support and ear clips of *A. swainsonii*. We warmly thank Hannah Maloney (QUT) for her sterling help on successive field trips in search of the elusive *A. vandycki* sp. nov. on Tasman Peninsula and typotypic *A. mimetes* from the chilly heights of Ebor. Billie Lazenby (DPIPWE) kindly provided ear clips of Tasmanian *A. swainsonii* and *A. vandycki* sp. nov. and her PhD trapping data for *A. vandycki* sp. nov. was invaluable. ABRS (Aus. Govt) funded the trip led by TYM to the Tasmania wilderness areas. QUT supported AMB's sabbatical, where he spent a month happily ensconced in the British Museum of Natural History's extensive type collection. AMB thanks David Maynard and Craig Reid (QVM, Launceston) for making him welcome and providing unreserved access to their antechinus collection. AMB thanks Heather Janetzki (QM) for expertly crafting the type and study skins of *A. vandycki* sp. nov., *A. swainsonii*, *A. mimetes* and *A. arktos* and for her help in acquiring loans generously provided by staff at MVic and the AM. We thank two anonymous reviewers who made very useful comments on the manuscript.

LITERATURE CITED

Archer, M. 1974. The development of cheek teeth in *Antechinus flavipes* (Marsupialia, Dasyuridae). *Journal of the Royal Society of Western Australia* **57**: 54-63.

1976. The dasyurid dentition and its relationships to that of didelphids, thylacinids, borhaenids (Marsupicarnivora) and peramelids (Peramelina: Marsupialia). *Australian Journal of Zoology Supplementary Series* **39**: 1-34.

Armstrong, L.A., Krajewski, C. & Westerman, M. 1998. Phylogeny of the dasyurid marsupial genus *Antechinus* based on cytochrome-b, 12S-rRNA, and protamine-P1 genes. *Journal of Mammalogy* **79**: 1379–1389 (http://dx.doi.org/10.2307/1383028).

Baker, A.M., Mutton, T.Y. & Hines, H.B. 2013. A new dasyurid marsupial from Kroombit Tops, south-east Queensland, Australia: the Silver-headed Antechinus, *Antechinus argentus* sp. nov. (Marsupialia: Dasyuridae). *Zootaxa* **3746**(2): 201–239 (http://dx.doi.org/10.11646/zootaxa.3746.2.1).

Baker, A.M., Mutton, T.Y., Hines, H.B. & Van Dyck, S. 2014. The Black-tailed Antechinus, *Antechinus arktos* sp. nov.: a new species of carnivorous marsupial from montane regions of the Tweed Volcano caldera, eastern Australia. *Zootaxa* **3765**(2): 101-133 (http://dx.doi.org/10.11646/zootaxa.3765.2.1).

Baker, A.M., Mutton, T.Y. & Van Dyck, S. 2012. A new dasyurid marsupial from eastern Queensland, Australia: the Buff-footed Antechinus, *Antechinus mysticus* sp. nov. (Marsupialia: Dasyuridae). *Zootaxa* **3515**: 1-37.

Baker, A.M., & Van Dyck, S. 2012. Taxonomy and redescription of the Fawn Antechinus, *Antechinus* *bellus* (Thomas) (Marsupialia: Dasyuridae). *Zootaxa* **3613**: 201-228.

2013a. Taxonomy and redescription of the Yellow-footed Antechinus, *Antechinus flavipes* (Waterhouse) (Marsupialia: Dasyuridae). *Zootaxa* **3649**: 1-62 (http://dx.doi.org/10.11646/zootaxa.3649.1).

2013b. Taxonomy and redescription of the Atherton Antechinus, *Antechinus godmani* (Thomas) (Marsupialia: Dasyuridae). *Zootaxa* **3670**: 401-439 (http://dx.doi.org/10.11646/zootaxa.3670.4.1).

Baverstock, P.R., Archer, M., Adams, M, & Richardson, B.J. 1982. Genetic relationships among 32 species of Australian dasyurid marsupials. Pp. 641–650. *In* Archer M, (ed) *Carnivorous marsupials*. (Royal Zoological Society of New South Wales: Sydney).

Crowther, M.S. 2002. Morphological variation within *Antechinus agilis* and *Antechinus stuartii* (Marsupialia : Dasyuridae). *Australian Journal of Zoology* **50**: 339–356 (http://dx.doi.org/10.1071/ZO01030).

Davison, A. 1986. Dentition of Victorian *Antechinus* species. *Australian Mammalogy* **9**: 73-85.

1991. A new subspecies of dusky antechinus, *Antechinus swainsonii* (Marsupialia: Dasyuridae) from western Victoria. *Australian Mammalogy* **14**: 103-113.

Dickman, C.R. 1982. Some ecological aspects of seasonal breeding in *Antechinus* (Dasyuridae, Marsupialia). Pp. 139-150. *In* Archer, M. (ed) *Carnivorous Marsupials*. (Royal Zoological Society of New South Wales: Sydney).

1986a. An experimental manipulation of the intensity of interspecific competition: effects on a small marsupial. *Oecologia* **70**(4): 536-543.

1986b. An experimental study of competition between two species of dasyurid marsupials. *Ecological Monographs* **56**: 221–241.

1988a. Body size, prey size, and community structure in insectivorous mammals. *Ecology* **69**(3): 569-580.

1988b. Sex ratio variation in response to interspecific competition. *The American Naturalist* **132**(2): 289-297.

2008. Dusky Antechinus *Antechinus swainsonii*. Pp. 99-100. *In,* Van Dyck, S. & Strahan, R. (eds) *Mammals of Australia (3rd edition)*. (New Holland: Australia).

Dickman, C.R., Parnaby, H.E., Crowther, M.S. & King, D.H. 1998. *Antechinus agilis* (Marsupialia : Dasyuridae), a new species from the A. stuartii complex in south-eastern Australia. *Australian Journal of Zoology* **46**(1): 1 – 26.

Firestone, K.B., Elphinstone, M.S., Sherwin, W.B. & Houlden, B.A. 1999. Phylogeographical population structure of tiger quolls Dasyurus maculatus (Dasyuridae: Marsupialia), and endangered carnivorous marsupial. Molecular Ecology **8**: 1613-1625.

Geoffroy [Saint-Hilaire], E. 1803. Note sur les espece du genre dasyure. *Bulletin des Sciences par la Societe Philomathique de Paris* **3**(81): 258-259.

Gibson, L.A., Wilson, B.A., Cahill, D.M. & Hill, J. 2004. Modelling suitable habitat of the swamp antechinus (*Antechinus minimus maritimus*) in the coastal heathlands of southern Victoria, Australia. *Biological Conservation* **117**: 143-150.

Gongora, J., Swan, A.B., Chong, A.Y., Ho, S.Y.W., Damayanti, C.S., Kolomyjec, S., Grant, T., Miller, E., Blair, D., Furlan, E. & Gust, N. 2012. Genetic structure and phylogeography of platypuses revealed by mitochondrial DNA. *Journal of Zoology* **286**(2012): 110–119.

Green, R.H. 1972. *The murids and small dasyurids in Tasmania. Parts 5 and 6*. Records of the Queen Victoria Museum No. 46.

Hall, T.A. 1999. BioEdit: a user-friendly biological sequence alignment editor and analysis program for Windows 95/98/NT. *Nucleic Acids Symposium Series* 41:95-98.

Happold, D.C.D. 1989. Small mammals of the Australian Alps. Pp.221–239 *In* Good, R. (ed) *The scientific significance of the Australian Alps*. (Australian Alps National Parks Liason Committee and Australian Academy of Science).

2011. Reproduction and ontogeny of *Mastacomys fuscus* (Rodentia: Muridae) in the Australian Alps and comparisons with other small mammals living in alpine communities. *Mammalian Biology* **76**(2011): 540–548.

Higgins, E.T. & Petterd, W.F. 1882. Descriptions of hitherto undescribed *Antechini* and *Muridae* inhabiting Tasmania. *Papers and Proceedings of the Royal Society of Tasmania* 171-176.

1883. New species of Antechini and Mus. *Papers and Proceedings of the Royal Society of Tasmania* 184-186.

1884. Descriptions of new Tasmanian animals. *Papers and Proceedings of the Royal Society of Tasmania* 181-185.

Iredale, T. & Troughton, E. 1934. A check-list of the mammals recorded from Australia. *Memoirs of the Australian Museum* **6**: 1–122.

Krajewski, C., Young, J., Buckley, L., Woolley, P.A. & Westerman, M. 1997. Reconstructing the Evolutionary Radiation of Dasyurine Marsupials with Cytochrome *b,* 12S rRNA, and Protamine P1 Gene Trees. *Journal of Mammalian Evolution* **4**(3): 217-236 (http://dx.doi.org/10.1023/A:1027349725642).

Lazenby B.T. & Dickman, C.R. 2013. Patterns of Detection and Capture Are Associated with Cohabiting Predators and Prey. *PLoS ONE* **8**(4): e59846.

Lunney, D., Matthews, A. & Grigg, J. 2001. The diet of *Antechinus agilis* and *A. swainsonii* in unlogged and regenerating sites in Mumbulla State Forest, south-eastern New South Wales. *Wildlife Research* **28**: 459–464 (http://dx.doi.org/10.1071/WR00015).

Macleay, W.S. 1841. Notice of a new genus of Mammalia discovered by J. Stuart, Esq., in New South Wales. *Annals and Magazine of Natural History* **8**: 241-243.

Mahoney, J.A. & Ride, W.D.L. 1988. Dasyuridae. Pp. 14-33. *In* Walton, D.W. (ed), `*Zoological Catalogue of Australia'. Vol. 5*. (Australian Government Publishing Service: Canberra).

Marlow, B. 1961. Reproductive behaviour of the marsupial mouse, *Antechinus flavipes* (Waterhouse) (Marsupialia) and the development of the pouch young. *Australian Journal of Zoology* **9**: 203–220 (http://dx.doi.org/10.1071/ZO9610203).

McAllan, B. 2003. Timing of reproduction in carnivorous marsupials. Pp. 147–168. *In* Jones, M., Dickman, C. & Archer, M. (eds). *Predators with Pouches: the Biology of Carnivorous Marsupials*. (CSIRO Publishing:Victoria).

McAllan, B., Dickman, C.R. & Crowther, M.S. 2006. Photoperiod as a reproductive cue in the marsupial genus *Antechinus:* ecological and evolutionary consequences. *Biological Journal of the Linnean Society* **87**: 365–379 (http://dx.doi.org/10.1111/j.1095-8312.2006.00571.x).

Menkhorst, P. (ed.) 1995. *Mammals of Victoria*. (Oxford University Press Australia: Melbourne).

Mutton, T.Y. 2011. *Systematics and Evolution of the Dasyurid Marsupial Genus* Antechinus. Honours Thesis, QUT: Brisbane, (Unpub.) 65 pp.

Nylander, J.A.A. 2004. MrModeltest v2. Program distributed by the author. Evolutionary Biology Centre, (Uppsala University).

Page, R.D.M. 1996. TREEVIEW: An application to display phylogenetic trees on personal computers. *Computer Applications in the Biosciences* **12**: 357-358.

Ridgway, R. 1912. *Colour Standards and Nomenclature*. (Published by the Author: United States National Museum).

Ronquist, F. & Huelsenbeck, J.P. 2003. MRBAYES 3: Bayesian phylogenetic inference under mixed models. *Bioinformatics* **19**: 1572–1574 (http://dx.doi.org/10.1093/bioinformatics/btg180).

Sale, M.G., Ward, S.J. & Arnould, J.P.Y. 2006. Aspects of the ecology of swamp antechinus (*Antechinus minimus maritimus*) on a Bass Strait island. *Wildlife Research* **33**:215-221 (http://dx.doi.org/10.1071/WR05051).

Sanecki, G.M., Green, K., Wood, H., Lindenmayer, D. & Sanecki, K.L. 2006. The influence of snow cover on home range and activity of the bush-rat (*Rattus fuscipes*) and the dusky antechinus (*Antechinus swainsonii*). *Wildlife Research* **33**: 489-496 (http://dx.doi.org/10.1071/WR05012).

Smith, A.M.A. 1983. The subspecific biochemical taxonomy of *Antechinus minimus, A. swainsonii* and *Sminthopsis leucopus* (Marsupialia: Dasyuridae). *Australian Journal of Zoology* **32**: 753-762 (http://dx.doi.org/10.1071/ZO9830753).

StatSoft, Inc. 2004. STATISTICA (data analysis software system), version 7.

Tamura, K., Stecher, G., Peterson, D., Filipski, A. & Kumar, S. 2013. MEGA6: Molecular Evolutionary Genetics Analysis Version 6.0. *Molecular Biology and Evolution* **30**:2725-2729 (http://dx.doi.org/10.1093/molbev/mst197).

Tate, G.H.H. 1947. Results of the Archbold Expeditions. No. 56. On the anatomy and classification of the Dasyuridae (Marsupialia). *Bulletin of the American Museum of Natural History* **88**: 101-155.

Thomas, M.O. 1888. *Catalogue of Marsupialia and Monotremata in the Collection of the British Museum*. (British Museum Natural History: London).

Thomas, O. 1904. On a collection of mammals made by Mr. J.T. Tunney in Arnhem Land, Northern Territory of South Australia. *Novitates Zoologicae* **11**: 222–229.

Thomas, M.O. 1924. A new Pouched Mouse (*Phascogale*) from northern New South Wales. *Annals and Magazine of Natural History* **9**(14): 528 (http://dx.doi.org/ 10.1080/00222932408633152).

Van Dyck, S. 1980. The Cinnamon Antechinus, *Antechinus leo* (Marsupialia: Dasyuridae), a new species from the vine-forests of Cape York Peninsula. *Australian Mammalogy* **3**: 5-17.

Van Dyck, S. 1997. Revisionary studies in *Murexia* and *Antechinus* (Marsupialia: Dasyuridae). Unpublished PhD Thesis, University of New South Wales, Australia.

Van Dyck, S. 2002. Morphology-based revision of *Murexia* and *Antechinus* (Marsupialia: Dasyuridae). *Memoirs of the Queensland Museum* **48**: 239-330.

Van Dyck, S.M. & Crowther, M.S. 2000. Reassessment of northern representatives of the *Antechinus stuartii* complex (Marsupialia: Dasyuridae): *A. subtropicus* sp. nov. and *A. adustus* new status. *Memoirs of the Queensland Museum* **45**(2): 611–635.

Van Dyck, S., & Ogilvie, P. 1977. *Antechinus swainsonii* (Waterhouse, 1840), the dusky marsupial mouse, an addition to the mammal fauna of Queensland. *Memoirs of the Queensland Museum* **18**: 69–73.

Wakefield, N.A. & Warneke, R.M. 1963. Some revision in *Antechinus* (Marsupialia) 1. *Victorian Naturalist* **80**: 192-219.

Waterhouse, G.R. 1840. Description of a new marsupial mammal belonging to the genus *Phascogale*. *Magazine of Natural History* **2**(4): 299.

Williams, R. & Williams, A. 1982. The life cycle of *Antechinus swainsonii* (Dasyuridae, Marsupialia). Pp. 91–95. *In* Archer, M. (ed), *Carnivorous Marsupials*. (Royal Zoological Society of New South Wales: Sydney, Australia).

Wilson, B. A., Aberton, J. & Reichl, T. 2001. Effects of fragmented habitat and fire on the distribution and ecology of the Swamp Antechinus (*Antechinus minimus maritimus*) in the Eastern Otways, Victoria. *Wildlife Research* **28**: 527–36 (http://dx.doi.org/10.1071/WR00016).

Wilson, B.A. & Bachmann, M.R. 2008. Swamp Antechinus *Antechinus minimus*. Pp. 93-94. *In* Van Dyck, S. and Strahan, R. (eds) *Mammals of Australia (3rd edition)*. (New Holland: Australia).

Woolley, P.A. 1966. Reproduction in *Antechinus* spp. and other dasyurid marsupials. *Symposia of the Zoological Society of London* **15**: 281–294.